CRREL REPORT 95-8

CRREL

Permafrost Formation Time

Virgil J. Lunardini

April 1995

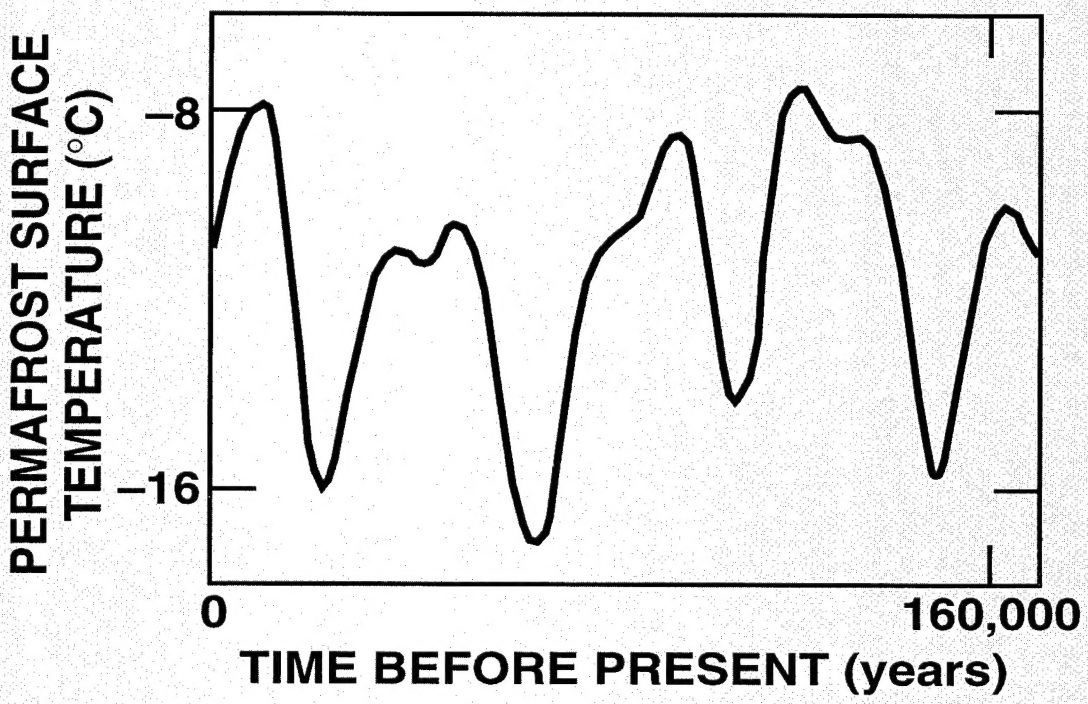

Abstract

The age of permafrost is closely linked to the time required for soil systems to freeze, since the permafrost must be at least as old as the formation time. Cycles of freeze–thaw will complicate the relation between the freeze rate and the age. A model based on pure conduction heat transfer with freeze–thaw is used to predict the time required for a given thickness of permafrost to develop, either heterogenetically or syngenetically. The formation time is a function of the long-term geothermal gradient (initial temperature of the thawed soil), the ratios of the frozen to thawed thermal properties, and the temperature history of the upper surface of the permafrost (higher than the air temperature). The simple theory allows universal graphs to be produced that predict the formation time for a given thickness of permafrost. Realistic soil property ratios and paleotemperature scenarios will then lead to estimates of the formation time of permafrost for a specific site. The model indicates that deep permafrost (more than 1500 m) requires formation times on the order of the complete Quaternary Period.

Cover: Reconstruction of paleotemperature history of Prudhoe Bay, Alaska (after Osterkamp and Gosink 1991).

For conversion of SI units to non-SI units of measurement consult *Standard Practice for Use of the International System of Units (SI)*, ASTM Standard E380-93, published by the American Society for Testing and Mater-ials, 1916 Race St., Philadelphia, Pa. 19103.

CRREL Report 95-8

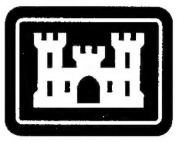

US Army Corps of Engineers
Cold Regions Research & Engineering Laboratory

Permafrost Formation Time

Virgil J. Lunardini

April 1995

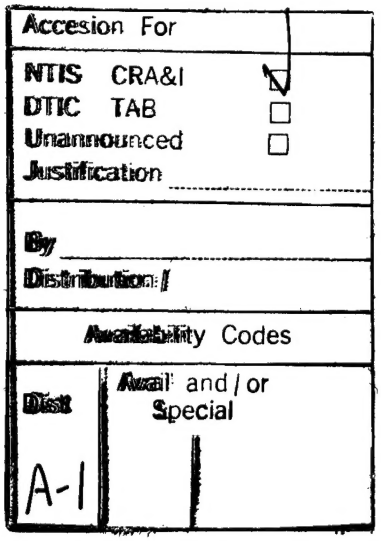

Prepared for
OFFICE OF THE CHIEF OF ENGINEERS

PREFACE

This report was prepared by Dr. Virgil J. Lunardini, Mechanical Engineer, Applied Research Division, Research and Engineering Directorate, U.S. Army Cold Regions Research and Engineering Laboratory. This study was primarily funded by U.S. Army Strategic Environmental Research and Development Program, *Deep Permafrost Borehole Sites in Alaska*, 2 6.00 78 203, and DA Project 4A161102AT24, Task BS/0045, *Climate Impacts on Permafrost Distribution and Integrity.*

The author thanks Dr. Gary Phetteplace and Michael Ferrick of CRREL for their technical review of this report.

CONTENTS

Preface ii
Nomenclature v
Introduction 1
  Origin and existence of permafrost 2
  Paleotemperatures 2
Theory 6
  Heterogenetic freeze relations 7
  Heterogenetic model verification 10
  Sensible and latent heats 10
  Neumann solution 11
  Steady-state solution 11
  Effect of quaternary freeze–thaw cycles 11
  Syngenetic growth of permafrost 12
  Syngenetic model verification 14
Discussion 14
  Prudhoe Bay, Alaska 18
  Deep permafrost 19
Conclusions 20
Literature cited 20
Appendix A: Soil properties and ratios 23
Appendix B: Quaternary cyclic thermal modulation 25
Appendix C: Heat balance integral equations for syngenetic permafrost growth 29
Appendix D: Energy flows at the permafrost base 35
Appendix E: FORTRAN programs for numerical quadrature of energy equation 39
Abstract 45

ILLUSTRATIONS

Figure

1. Paleotemperature variations 3
2. Pleistocene temperature fluctuations 3
3. Vostok ice core temperature inferences 4
4. Permafrost surface paleotemperature model for Prudhoe Bay, Alaska 4
5. Permafrost surface paleotemperature model for East Siberian location 5
6. Reconstructed temperature for northern China during last ice age 5
7. Mean paleotemperature departure, Prudhoe Bay, Alaska, during one glacial cycle 5
8. Paleotemperature history at Mackenzie Delta, Canada 6
9. Freeze of a semi-infinite region with linear initial temperature 7
10. Temperature distribution after initial freeze of soil 11
11. Bottom thaw of permafrost 12
12. Thermal state at end of melting and long-term equilibrium 12
13. Geometry and coordinate system for freeze of a semi-inifinite medium with moving upper surface 12

Figure

14. Coordinate system for stationary upper surface 13
15. Formation time of permafrost, saturated mineral soils, $\phi = 0$, $\varepsilon = 0.4$ 15
16. Formation time of permafrost, saturated mineral soils, $\phi = 0$, $\varepsilon = 0.379$ 15
17. Formation time of permafrost, saturated mineral soils, $\phi = 0$, $\varepsilon = 0.3$ 16
18. Formation time for permafrost to reach 90% equilibrium thickness, saturated mineral soils 16
19. Effect of soil porosity on permafrost thickness after 15,000 years, saturated soils, $G = 0.0286$°C/m 16
20. Syngenetic growth of permafrost, saturated mineral soils, $\phi = 0$, $\varepsilon = 0.379$, $S_T = 0.15$ 17
21. Syngenetic growth of permafrost, saturated mineral soils, $\phi = 0$, $\varepsilon = 0.379$, $\psi = 0.15$ 17
22. Growth of permafrost at Prudhoe Bay, Alaska 19

TABLES

Table

1. Movement of T_f isotherm, homogeneous soil for heterogenetic freezing 10
2. Movement of T_f isotherm, homogeneous soil for syngenetic freezing 14
3. Paleotemperature scenarios, Prudhoe Bay, Alaska 17
4. Effect of previous cooling on permafrost growth time 19
5. Formation time of deep permafrost 19
6. Extreme predicted permafrost thickness 20

NOMENCLATURE

c	specific heat
c_{12}	c_1/c_2
C	ρc, volumetric specific heat
f	fraction of geothermal energy used for melt
g	$\frac{\alpha_{21}(1+\sigma)}{\beta[(\beta+2)\sigma+2]}+1$
g'	$dg/d\sigma$
G	geothermal gradient (slope of initial temperature distribution)
k	thermal conductivity
k_g	thermal conductivity of soil solids
k_{12}	k_1/k_2
ℓ	latent heat of solidification
L	$\rho\ell$, volumetric latent heat
M	$m^2\pi^2 t/4t_c$
q_g	geothermal energy flow
Q_S, Q_L	sensible and latent heats
S	soil saturation parameter
S_T	$\frac{c_1}{\ell}(T_1 - T_s)$, Stefan Number
t	time
t_c	$X_o^2/4\alpha_f$, characteristic time for permafrost temperature changes
t_m	time to complete melt of permafrost
T	temperature
U	deposition rate at surface of permafrost
x	depth coordinate
x_w	volumetric water content
X	permafrost thickness
α	thermal diffusivity
α_{12}	α_1/α_2
β	δ/X
β'	$\frac{d\beta}{d\sigma}$
δ	depth of temperature disturbance
ε	soil porosity
γ_N	$X/2\sqrt{\alpha_1 t}$
ΔT	$T_o - T_f$
ΔT_1	$T_f - T_s$
ξ	integrated temperature
ρ	density
σ	$\frac{G}{\Delta T_1}X$
σ_N	dimensionless freeze depth for Neumann solution
τ	$\alpha_1\left(\frac{G}{\Delta T_1}\right)^2 t$
ϕ	$\frac{T_o - T_f}{T_f - T_s}$
ψ	$\frac{U\Delta T_1}{G\alpha_1}$

Subscripts

f	solidification or freeze value
e	equilibrium value
i	initial value
o	initial surface value
s	surface
u	thawed
1,2	frozen and thawed, respectively
∞	steady-state value

Permafrost Formation Time

VIRGIL J. LUNARDINI

INTRODUCTION

The age of permafrost is of interest to biologists, geophysicists and engineers. Clearly, permafrost must be at least as old as the time it took for it to form; thus, the formation time of permafrost can be considered its minimum age. A volume of permafrost can be much older than this since it may exist for many years after formation. This report will examine the formation time of permafrost using a pure heat conduction model. As we shall see, the surface temperature history of the soil mass is critical for any prediction of the permafrost formation time. Since the formation time of permafrost is expected to be on the order of millennia, it is necessary to examine the geophysical record to obtain some bounds on realistic surface temperatures that the Earth has experienced during the time when permafrost was growing. First, we will discuss permafrost and paleotemperature scenarios, then we will formulate a mathematical model of permafrost growth, and, finally, we will examine some predictions by the model of permafrost formation times.

Permafrost is a widespread phenomenon that has been and still is greatly misunderstood. The term "permafrost" is generally attributed to S.W. Muller (1945), who apparently coined the name in place of the more awkward terms: permanently frozen ground or permanent frost. Bryan (1946) suggested the term "pergelisol," but this has not been adopted except in the French literature. In order to understand the concept, let us look at a general definition given in Lunardini (1981a):

> Permafrost describes the thermal condition of earth materials (sand, glacial till, organic matter, etc.) when their temperature remains at or below 32°F (0°C) continuously for a significantly long time, but not necessarily for an entire geological period. It does not include earth materials that drop below 32°F during one winter and remain below 32°F through the following summer and into the next winter, although for practical engineering purposes such materials may be included.

Clearly, permafrost is not so much a material as it is the thermal state of ordinary soil systems. It does not include systems that are at or below 0°C, but contain no earth materials, e.g., ice caps, glaciers and icebergs. There is no agreement on the minimum time during which the material must remain below 0°C to qualify as permafrost. Soils that freeze during an exceptionally severe winter and survive for 1 or 2 more years are called "pereletoks," and often are not classified as permafrost (Swinzow 1969).

The existence of permafrost is a result of the history and the present state of the energy balance at the Earth's surface—measured by the surface temperature—and the deep Earth heat flow. If permafrost exists and the net yearly gain of energy by the entire permafrost volume is equal to the net loss of energy, then the permafrost will remain stationary, while an excess heat gain over heat loss will result in a net loss of frozen material. Given the same energy balances, however, i.e., net gain of energy over the year, one region may have permafrost (albeit degrading) while another will not. This is ascribable to the thermal history of the frozen ground in the two areas. Though both are losing or have lost permafrost, one region may have started with a larger volume of permafrost than the other. Thus, the present energy flow conditions may be such that permafrost cannot exist in one region, whereas it will subsist in another area, although in a receding form often referred to as "relic permafrost."

In this sense previous glaciation has very likely played an important role in the present existence of permafrost in marginal areas. It is safe to conclude that little, if any, permafrost exists beneath nonpolar glaciers, but once they withdraw, permafrost may rapidly form and grow. So, previously glaciated regions will show a lesser volume of frozen ground than unglaciated regions with similar climatic histories. In this regard it is significant that Canada was heavily glaciated while Russia (Siberia) had little permanent glaciation. Thus, the permafrost thickness in Siberia is much greater than in Canada, although the climates are similar.

Since the energy balance involves meteorological conditions, surface vegetation, topography and soil conditions, we can anticipate that we will find no simple correlation for the existence of permafrost in the marginal or discontinuous regions. Permafrost does exist far south of the usually accepted limits in scattered patches almost always associated with high altitudes and, thus, microclimates similar to the usual permafrost regions.

Origin and existence of permafrost

In discussing the present distribution of permafrost, questions often arise concerning its origin and age. These two concepts should be clearly differentiated, since they deal with two separate phenomena. The age of a particular deposit of permafrost is the time that has elapsed since the freezing of the soil system. Actually, it may be very difficult or impossible to determine this age because thawing and freezing may cycle at long intervals and different frequencies in different regions of the Earth. Thus, the ages of two "similar" deposits of permafrost may be quite different. In this regard, the presence of preserved animal remains may be a reliable clue to the age of a deposit of frozen ground. The age of permafrost is a question of significance and may be useful to paleontologists, paleobotanists, etc. The present thermal state of the permafrost—temperature, degradation, aggradation, etc.—is of interest to engineers.

The origin of permafrost involves the question of the conditions under which it can form and grow. These same conditions will explain the present existence of permafrost at a given location. As the conditions for the origin of permafrost are dynamic, it is certainly possible that areas now lacking permafrost once had these underlying frozen strata, and that the present regions of permafrost could once have been thawed. In other words, the present existence of permafrost depends upon two things: the proper energy exchange conditions and the thermodynamic state of the permafrost mass itself. The first of these conditions has little to do with past climatic conditions, but the second is a function of the complete thermal history of the permafrost and is thus related to past climate. In this sense, it is incorrect to describe permafrost simply as a legacy of the last great ice age. It is possible that some, perhaps most, permafrost had its origin at the beginning of the Pleistocene era (Brown 1964), but this should not imply that the intervening thermal conditions were without significance.

From the above discussion, it should be clear that the formation and existence of permafrost are related to the present and historical conditions of energy exchange between the soil and the atmosphere. Nevertheless, it is not possible to state these conditions in a simple, precise manner that will allow us to define unique permafrost indicators.

Over a sufficiently long time span, the energy exchange will be periodic, and, averaged over a number of periods, the net energy flow for a given soil volume will determine its thermodynamic state. Dynamic equilibrium of the energy flows may exist such that the soil is perennially frozen or the thermodynamic state of the soil may be varying because of an imbalance of the cyclic energy flows. The original formation of permafrost depends upon a net periodic (yearly) loss of energy from the soil volume that must persist for many, many years for the permafrost to attain great thicknesses. The maintenance of the present thermodynamic state of permafrost requires only that the net energy flow averaged over a number of years be zero.

Paleotemperatures

The thermal history of permafrost is greatly influenced by the long-term temperature variations experienced at its upper surface. The relative mean global temperature deduced from oxygen isotope data is shown for the past 180 million years in Figure 1 (Eddy and Bradley 1991). There was probably little or no permafrost prior to the late Tertiary Period and certainly none for 100 million years prior to the long-term cooling

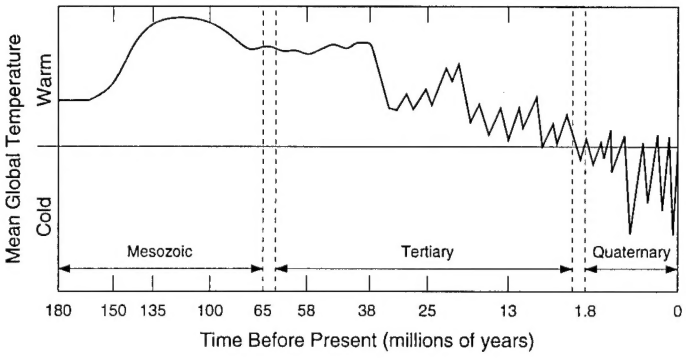

Figure 1. Paleotemperature variations (after Eddy and Bradley 1991).

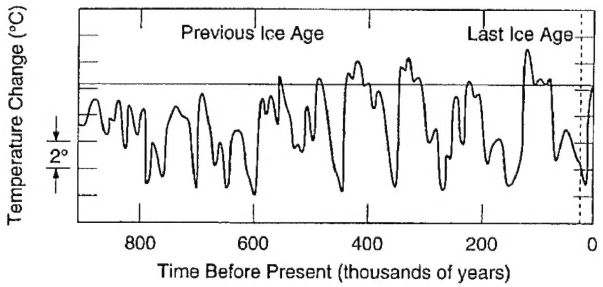

Figure 2. Pleistocene temperature fluctuations (after Folland et al. 1990).

that began 35 million years before present. During the Pliocene, some 2–5 million years before present, the temperature oscillated 0–4°C above the present values. Permafrost was probably present at locations that now have mean temperatures less than –14°C but with greatly reduced thickness and quite variable temporal existence.

The Quaternary Period, which includes the Pleistocene (about 1 million years) and the Holocene (present to about 10,000 years), remains a time of greatly reduced temperatures and massive glaciations. The period is marked by ice ages of 100,000 to 120,000 years duration, interrupted by interglacials, and with increasingly severe minimum temperatures and temperature drops. We are now in the Holocene interglacial (which is actually cooler than the previous interglacial, the Sangamon or Eem) and the record would seem to indicate the next significant temperature move should be downward with a new ice age evolving. Figure 2 shows the temperature record (again from isotope analysis) for the past million years or so (Folland et al. 1990). We note graphically the record of at least four or five glacial periods, with the last one ending some 12,000 years ago in North America—the Wisconsin. The temperatures variations from present values swung from highs of +3°C during interglacials to lows of about –10°C during the glacial maximums of the last million years. The overall trends reveal very rapid temperature rises over time spans of approximately 12,000–13,000 years, followed by less rapid temperature drops over 20,000 years, followed by a period of about 100,000 years of gradually decreasing temperatures with interglacial temperature rises of 4°C.

The temperature history of the past 160,000 years has been quantified using the deep glacial ice cores taken in Greenland and Antarctica. Figure 3 shows the temperature variations from present values, for the time of the last great ice age, taken from the isotope analysis of the Vostok (Antarctic) core (Jouzel et al. 1987). The maximum temperature excess of the past 160,000 years was about 3°C and thus only the discontinuous permafrost zones would have been in danger of disappearing, although there was continual change in the permafrost thickness. If we assume that the temperature variations obtained from the ocean isotope and ice core analyses are global, then the paleotemperature history at a specific site can be reconstructed using the present temperature data. This has been done for Prudhoe Bay by Osterkamp and Gosink (1991) as shown in Figure 4 and for East Siberia by Maximova and Romanovsky (1988) (Fig. 5). Sun and Li (1988) also presented a quantitative model of temperature fluctuations during the last ice age in northern China (Fig. 6).

The isotopic data all indicate that the temperature at a given site could have dropped as much as 10 to

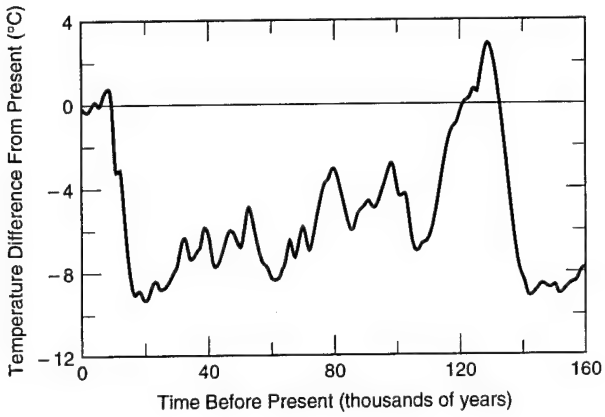

Figure 3. Vostok (Antarctica) ice core temperature inferences (after Jouzel et al. 1987)

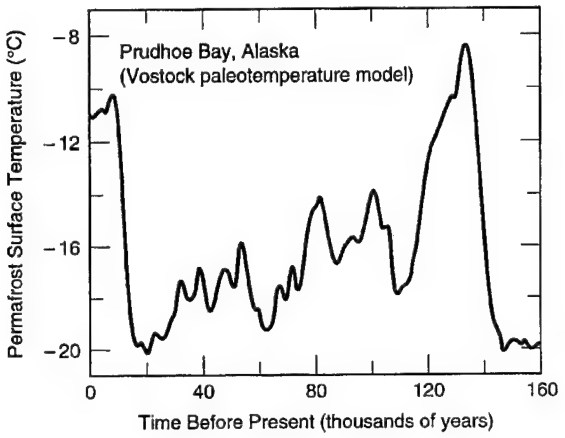

a. Based on Vostok (Antarctica) ice core temperature inferences.

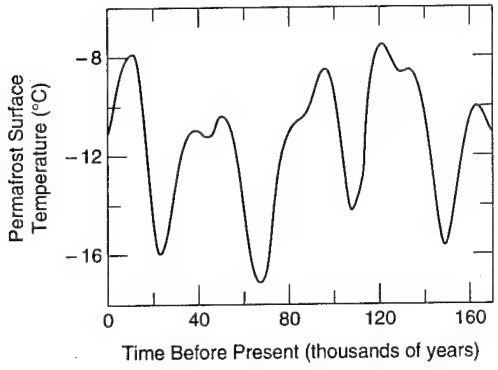

b. Based on East Siberia model.

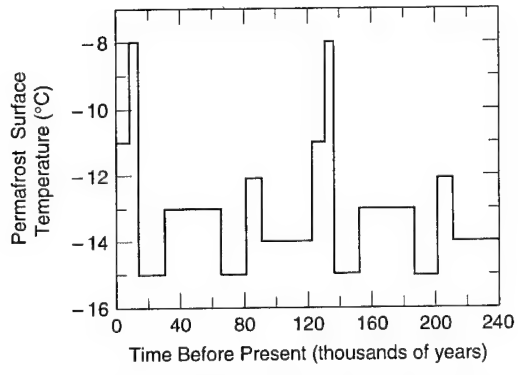

c. Based on Brigham and Miller (1983) data for Barrow, Alaska.

Figure 4. Permafrost surface paleotemperature model for Prudhoe Bay, Alaska (after Osterkamp and Gosink 1991).

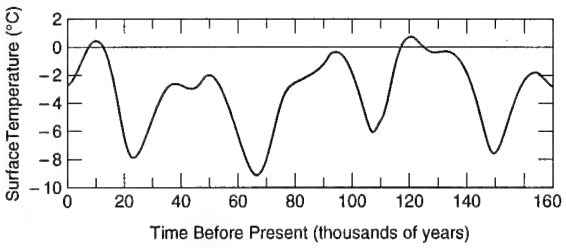

Figure 5. Permafrost surface paleotemperature model for East Siberian location (after Maximova and Romanovsky 1988).

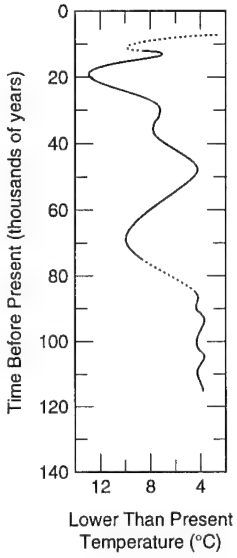

Figure 6. Reconstructed temperature for northern China during last ice age (after Sun and Li 1988).

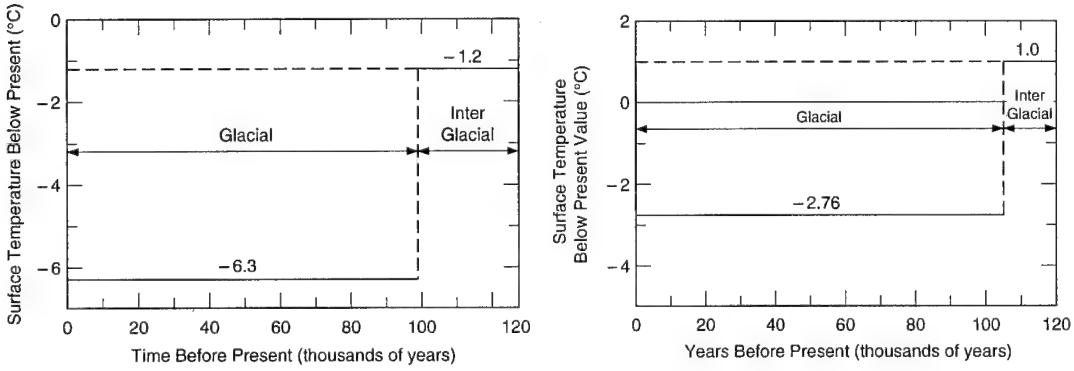

a. Based on Vostok (Antarctica) ice core data, $\Delta T = -5.29°C$.

b. Based on Brigham and Miller (1983) data, $\Delta T = -2.54°C$.

Figure 7. Mean paleotemperature departure, Prudhoe Bay, Alaska, during one glacial cycle.

12°C below the present values for varying periods of time. While extreme temperature drops at some sites may have been significantly greater than these values, there is no convincing evidence of this. Temperature variations of 8 to 12°C during the last glaciation have also been reported from the Greenland ice cores (Dansgaard and Oeschger 1989). Folland et al. (1990) note that global temperatures underwent 5–7°C variations, with changes as great as 10–15°C at middle and high latitude regions of the Northern Hemisphere. During the Eemian interglacial, temperatures in Siberia, Canada and Greenland may have increased by 4–8°C. Thus, it would seem prudent to use extremal paleotemperature excursions on this order of magnitude (10–12°C) for the development of permafrost formation models. We cannot ascribe the rapid growth of deep permafrost to extraordinarily low temperatures that are beyond the ranges we have mentioned above. Figure 7 shows two examples of average paleotemperatures for a glacial cycle made up of glacial and inter-

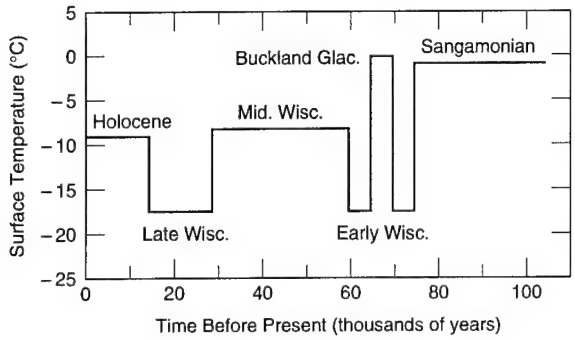

Figure 8. Paleotemperature history at Mackenzie Delta, Canada (after Allen et al. 1988).

glacial intervals. Figure 7a is based on the Vostok ice core while Figure 7b is calculated from information given by Brigham and Miller (1983) for Prudhoe Bay, Alaska.

There have been surprisingly few systematic thermal studies of the origin of permafrost and the total time required for its formation. Osterkamp and Gosink (1991) studied the response of permafrost thickness to surface temperature variations. They used quasi-steady and numerical models to predict the position of the permafrost bottom, with arbitrary initial permafrost thicknesses, but were interested in the inverse problem of deducing paleotemperatures from the present permafrost data at Prudhoe Bay, Alaska. Allen et al. (1988) used a quasi-steady model (which will inherently underpredict the growth time) for the same purpose in the Mackenzie Delta region of Canada, using still another paleotemperature history (Fig. 8). They assumed that Illinois permafrost was completely melted during the Sangamon interglacial, although this is highly unlikely given the time available, unless Illinoisian glaciation limited the permafrost thickness to modest values. Nevertheless, they used an initial permafrost thickness and predicted about 800 m of growth in 75,000 years. Their thermal model is based on the work of Lachenbruch et al. (1982) dealing with the rate of thaw of thick permafrost zones during several millennia. Romanovsky et al. (1988) noted qualitative aspects of the origin and disappearance of permafrost in the Transbaikal area of Russia. Katasonov (1988) used "cryogenic structures" to argue for the origin of permafrost early in the Quaternary and its persistence up to the present.

In this report an attempt is made to predict the rate of permafrost formation, starting with no permafrost, i.e., its origin, using a simple conduction model. If the soil forming the permafrost exists before freezing starts, the growth is heterogenetic. When the permafrost forms as the soil material is gradually deposited at the surface, the permafrost is said to have a syngenetic origin. The thermal conditions for each type of growth will be examined.

THEORY

The solution to conductive heat transfer problems, with solidification phase change, has interested engineers and mathematicians for over a century. These problems (often referred to as Stefan problems) are inherently nonlinear and solution methods are very restricted. A classical solution for the case of a constant temperature, semi-infinite medium that undergoes a step change of surface temperature was given by Neumann (1860) and expanded upon by Carslaw and Jaeger (1959); it is called the Neumann solution. Tao (1978) extended the similarity technique of Neumann to the semi-infinite slab with arbitrary initial temperature. This is precisely the solution we need, but unfortunately this exact solution is such that numerical computations are extremely difficult because of transient functions that require an increasing number of series terms as time increases. For permafrost formation the time scales are so huge that Tao's solution is impractical and cannot be used. Like the exact solution of Lozano and Reemsten (1981), for flux boundary conditions, Tao's solution is perhaps best used numerically to verify the accuracy of approximate and numerical solutions or for short-time solutions.

The search for practical solutions for engineering design has led to some convenient approximate solution methods for Stefan problems. The heat balance integral technique solves the energy equation on aver-

age over a space volume, instead of at each point of space (Goodman 1958). The concept is identical to the well-known momentum integral technique of fluid mechanics, sometimes referred as the Karman-Pohlhausen method (Schlichting 1968). The method has been applied successfully to constant initial temperature problems of the semi-infinite slab (Lunardini and Varotta 1981) as well as the cylindrical geometry (Lunardini 1980). A modification of the integral method utilizing a single integration over an entire nonconstant property volume has yielded accurate solutions (Yuen 1980, Lunardini 1981b,1982).

The integral solution has been used for a problem with variable initial temperature distributions, but the results were limited to shallow freeze depths (Lunardini 1984). This report presents an approximate solution to the modified Neumann problem for which a linear initial temperature distribution exists. Such an initial temperature is common for soil systems with a geothermal temperature gradient and is directly applicable to the question of permafrost formation rates.

Heterogenetic freeze relations

Figure 9 shows the case of an infinite layer of soil with a linear initial temperature distribution (G represents a geothermal gradient). The soil is assumed to be homogeneous and conduction is the only mode of energy transfer. At zero time the surface temperature drops to T_s and is held constant while freezing commences. At any time $t > 0$, there is a frozen layer, called layer 1 ($0 < x < X$) and a thawed layer ($x > X$). The thawed layer is further divided into layer 2 ($X < x < X + \delta$) where temperature changes occur and layer 3 ($x > X + \delta$) where thermal effects are not discernible. We ignore the finite time it takes for the surface temperature to drop to the freezing point, T_f. This time will be small compared to the formation time and a realistic scenario prior to the onset of freezing is $T_0 = T_f$.

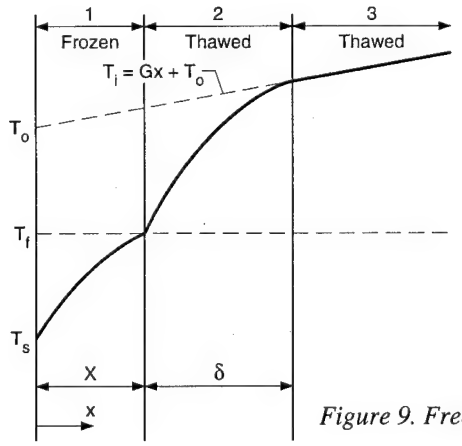

Figure 9. Freeze of a semi-infinite region with linear initial temperature.

The governing equations are the conduction energy equations with appropriate boundary and initial conditions; see the *Nomenclature* for definition of symbols not defined in the text.

For the frozen zone

$$\alpha_1 \frac{\partial^2 T_1}{\partial x^2} = \frac{\partial T_1}{\partial t} \qquad 0 \le x \le X \tag{1}$$

$$T_1 (X, t) = T_f \tag{1a}$$

$$T_1 (0, t) = T_s . \tag{1b}$$

For the thawed zone

$$\alpha_2 \frac{\partial^2 T_2}{\partial x^2} = \frac{\partial T_2}{\partial t} \qquad 0 \le x \le X + \delta \tag{2}$$

$$T_2(X,t) = T_f$$

$$\frac{\partial T_2(X+\delta,t)}{\partial x} = G. \tag{2b}$$

The initial temperature at the beginning of freeze is

$$T_i = T_o + Gx\,. \tag{2c}$$

The maximum depth at any time to which the temperature disturbance will be felt is $X + \delta$. Then

$$T_2(X+\delta,t) = (X+\delta)G + T_o. \tag{2d}$$

The energy balance at the phase change interface for the freeze process is

$$k_1\frac{\partial T_1}{\partial x}(X,t) - k_2\frac{\partial T_2}{\partial x}(X,t) = \rho_2\ell\frac{dX}{dt}\,. \tag{2e}$$

The energy balance at the freezing front can also be written as two equations (Lunardini 1981b)

$$-k_1\left[\frac{\partial T_1(X,t)}{\partial x}\right]^2 + k_2\frac{\partial T_2(X,t)}{\partial x}\frac{\partial T_1(X,t)}{\partial x} = \rho_1\ell\alpha_1\frac{\partial^2 T_1(X,t)}{\partial x^2} \tag{3}$$

$$-k_1\frac{\partial T_1(X,t)}{\partial x}\frac{\partial T_2(X,t)}{\partial x} + k_2\left[\frac{\partial T_2(X,t)}{\partial x}\right]^2 = \rho_2\ell\alpha_2\frac{\partial^2 T_2(X,t)}{\partial x^2}\,. \tag{4}$$

Because of the initial temperature distribution, during freeze the heat flow to the interface from the thawed region will exceed the geothermal heat flow until equilibrium is established. Likewise, during a thaw period the heat flow from the thawed zone will be less than the deep geothermal heat flow.

An approximate solution to this problem will be obtained using the heat balance integral technique (see Lunardini 1991). In this method, the differential equations are solved on average over a finite volume of material rather than at each point of the region. The integration of the energy equations over the regions where temperature changes are occurring, $0 \le x \le X + \delta$, detailed by Lunardini (1981b) is

$$\frac{d}{dt}\left\{\rho_1 c_1\int_0^X T_1(x,t)dx + \rho_2 c_2\int_X^{X+\delta} T_2(x,t)dx - \rho_1\ell X + (\rho_2 c_2 - \rho_1 c_1)T_f X\right.$$

$$\left. - \rho_2 c_2(X+\delta)\left[T_o + \frac{G}{2}(X+\delta)\right]\right\} = -k_1\frac{\partial T_1(0,t)}{\partial x} + k_2 G\,. \tag{5}$$

Quadratic temperature profiles in regions 1 and 2 that satisfy the boundary conditions are chosen as

$$T_1 = T_f + a_1 X\left(\frac{x-X}{X}\right) + (a_1 X - \Delta T_1)\left(\frac{x-X}{X}\right)^2 \tag{6}$$

$$T_2 = T_f + \left[G(\delta+2X) + 2\Delta T\right]\frac{x-X}{\delta} - \left(GX + \Delta T\right)\frac{(x-X)^2}{\delta^2} \tag{7}$$

where

$$a_1 X = \frac{\Delta T_1}{g}, g = \frac{\alpha_{21}(\Delta T + GX)X}{\delta\left[G(\delta + 2X) + 2\Delta T\right]} + 1.$$

In general, the simplest temperature profiles that will satisfy the boundary conditions should be chosen. The accuracy of the method increases as the order of a polynomial temperature choice increases; however, the use of high-order polynomials (third and higher) is often not justified since a small increase in accuracy requires significantly more computational effort. Equation 4 can be used to find a relation between X and d. In nondimensional form this is

$$\frac{\beta}{g} - k_{21}\left[\sigma(\beta + 2) + 2\phi\right] = \frac{2\rho_{21}\beta(g-1)}{S_T}. \tag{8}$$

Equation 5, the energy integral equation, can now be written nondimensionally, using eq 6 and 7 as

$$\tau = \int_0^\sigma K d\sigma \tag{9}$$

$$K = \frac{b_1 + b_2\beta - \frac{1}{6g}\left(1 - \frac{\sigma g'}{g}\right) - C_{21}\sigma\left(\frac{2}{3}\beta + 1\right) - \frac{C_{21}}{3}(\sigma + \phi)\sigma\beta'}{\frac{1}{\sigma}\left(\frac{1}{g} - 2\right) + k_{21}} \tag{10}$$

where

$$b_1 = -\left(\frac{1}{3} + \frac{1}{S_T} + C_{21}\phi\right)$$

$$b_2 = -\frac{1}{3}C_{21}\phi.$$

The derivatives of β and g can be found from the following equations

$$\frac{d\beta}{d\sigma} = \beta' = \frac{a_5 + a_1 a_4}{a_3 + a_2 a_4}. \tag{11}$$

$$\frac{dg}{d\sigma} = g' = a_1 - a_2\beta'. \tag{12}$$

where

$$a_1 = \frac{\alpha_{21}}{m}\left[1 - \frac{(\sigma + \phi)\,\beta(\beta + 2)}{m}\right]$$

$$a_2 = \frac{\alpha_{21}(\sigma + \phi)}{m^2}\left[2\sigma(\beta + 1) + 2\phi\right]$$

$$a_3 = \frac{1}{g} - \frac{2\rho_{21}(g-1)}{S_T} - k_{21}\sigma$$

$$a_4 = \left(\frac{2\rho_{21}}{S_T} + \frac{1}{g^2}\right)\beta$$

$$a_5 = k_{21}(\beta + 2)$$

$$m = \beta[\sigma(\beta + 2) + 2\phi].$$

The problem has now been reduced to a simple numerical quadrature of eq 9 using the auxiliary relations of eq 10–12. The numerical solution of eq 9 can be obtained quite easily with a personal computer and any standard numerical integration routine. (A FORTRAN program, PERM.FOR, to carry out the integration is listed in Appendix E.)

The model requires only the ratios of the thawed to frozen values of thermal conductivity, specific heat capacity and density for the permafrost soils. These property ratios can be estimated with good accuracy for soil systems as noted in Appendix A. The absolute values of the frozen and thawed soil properties are not needed to carry out the solution of eq 9–12.

Heterogenetic model verification

It is possible to check the solution for a special case. Although there is no exact solution for the phase-change case, a solution was found for the transient location of the T_f isotherm for a homogeneous soil with zero latent heat, i.e, infinite Stefan number (Lunardini, in prep.). The relation is

$$\operatorname{erf}\frac{X}{2\sqrt{\alpha t}} = 1 - \frac{GX}{T_f - T_s} \quad . \tag{13}$$

Table 1. Movement of T_f isotherm, homogeneous soil for heterogenetic freezing.
$S_T = 1000$, $\ell = 0$, $T_f - T_s = 10°C$, $\phi = 0$, $G = 0.0286°C/m$.

X	*Time (years)*		
(m)	*Eq 9*	*Exact eq 13*	*% difference*
27.97	2.08	2.15	3.6
69.93	22.63	25.30	10.6
139.86	204.48	234.73	12.9
314.69	53,053.2	48,141.3	–10.2
332.17	242,852.4	238,469.1	–1.8

If we let the Stefan number be large and hold the property ratios to unity, the approximate solution can be compared to this exact relation. Table 1 notes the results for a typical case.

The comparison indicates that the approximate technique gives good results, especially as the time increases. The results also show that the T_f isotherm requires surprisingly long times to penetrate deeply, even without phase change. This is explainable by the sensible-to-latent heat ratios to be examined below.

Sensible and latent heats

The total energy extracted from a unit area of soil is the sum of the latent and sensible energies.

$$Q_T = Q_L + Q_S \, . \tag{14}$$

The latent energy is

$$Q_L = X_L \tag{15}$$

while the sensible heat flow is

$$Q_S = C_f \int_0^X [T_f - T_1(x,t)]dx + C_u \int_0^X (T_i - T_f)\, dx + C_u \int_X^{X+\delta} [T_i - T_2(x,t)]\, dx \tag{16}$$

where $T_i\,(x)$ is the original temperature before the freeze starts. Using the temperature relations (eq 6 and 7) leads to

$$Q_S = C_f \Delta T_1 X\{C_{21}\,[(\sigma/2) + \phi + \beta(\sigma + \phi)/3] + (0.5/g + 1)/3\} \, . \tag{17}$$

The ratio of the sensible to the latent heat is

$$Q_S / Q_L = S_T \{C_{21}\,[(\sigma/2) + \phi + \beta(\sigma + \phi)/3] + (0.5/g + 1)/3\}. \tag{18}$$

This ratio is quite large even for small Stefan numbers and tends to increase as the freeze depth increases.

Neumann solution

The Neumann solution is a special case that occurs when the initial temperature gradient G is zero. Thus, it is the conduction solution that will predict the minimum time needed to form a given thickness of frozen material. The exact solution is well known as

$$X = 2\gamma_N \sqrt{\alpha_1 t}\,. \tag{19}$$

γ_N is a function of S_T, ϕ and the property ratios and is known (Lunardini 1981). Equation 19 can also be written as

$$\sigma_N = 2\gamma_N \sqrt{\tau}\,. \tag{20}$$

Steady-state solution

Unlike the Neumann solution, the permafrost zone for the general case with a non-zero geothermal gradient reaches an equilibrium value. The equilibrium value is the thickness of permafrost that will form if infinite time is available for growth. At steady state, the net heat flux at the phase change interface will be zero so that $(dX/dt)_\infty = 0$. Then the temperature in region 1 is

$$T_{1\infty} = \frac{\Delta T_1 x}{X_\infty} + T_s. \tag{21}$$

At the solidification interface

$$k_1 \frac{\partial T_{1\infty}}{\partial x} = k_2 G\,. \tag{22}$$

Thus

$$X_\infty = \frac{\Delta T_1}{k_{21} G} \tag{23}$$

or

$$\sigma_\infty = \frac{1}{k_{21}}. \tag{24}$$

Effect of quaternary freeze–thaw cycles

The previous discussion assumed that the soil was initially unfrozen, with a temperature distribution given by eq 2c, as shown in Figure 9. However, the cyclic warming and cooling that has taken place over the past million years will tend to cyclically lower the ground temperature as compared to the previous initial temperature distribution. If the temperature is lower than that of eq 2c, the permafrost growth will be accelerated. Figure 10 shows the thermal state of permafrost at equilibrium with a geothermal heat flow—the solid line. The approach to the equilibrium state of the permafrost is affected by the initial temperature of the soil in that the time to reach equilibrium will be greatly changed but the final equilibrium thickness is not affected by the initial assumption (see eq 23).

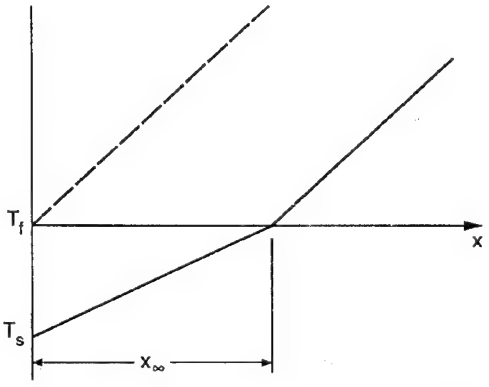

Figure 10. Temperature distribution after initial freeze of soil.

Let us assume that surface warming to T_f occurs and the permafrost eventually reaches a stage where the entire frozen zone is at T_f. The system starts to thaw in this condition and we ignore the time needed to reach this state (small compared to melt time scales) and also neglect the bottom freeze–thaw during this initial warming time. Figure 11 shows the thermal state as the bottom thaw commences, at $x = X_0$. The geothermal heat flow is used to melt permafrost and also to warm the soil in the region X

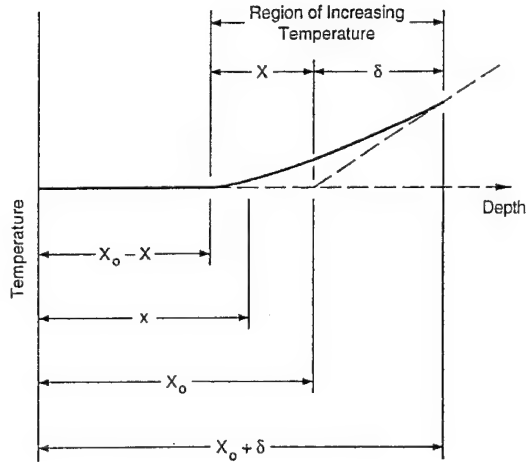

Figure 11. Bottom thaw of permafrost.

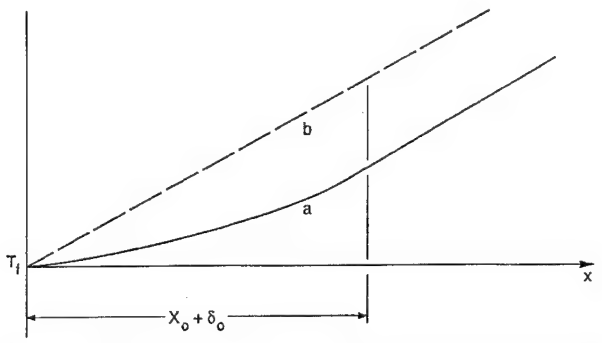

Figure 12. Thermal state at end of melting (a) and long-term equilibrium (b).

+ δ. The maximum thaw rate occurs if all of the geothermal heat flow goes into melting, but this is physically impossible.

Given sufficient time, the entire permafrost volume melts and the soil temperature is as shown in Figure 12—curve a. A layer of soil of thickness $X_o + \delta_o$ will be thermally modulated. The temperature gradient for depths greater than $X_o + \delta_o$ is G, the geothermal gradient. Also shown in Figure 12 is the dashed line (curve b) denoting the equilibrium temperature distribution with the same geothermal gradient but no cooling. This state would be reached if the surface remained at T_f for a long time after thaw was completed. Clearly, the sensible heat that must be removed in the modulated case (curve a) will be less than that for the original freeze discussed earlier (curve b). This means that cooled soil (after cyclic melting or warming) will freeze much faster with the same mean surface temperature. This temperature modulation will only be significant for zones of relatively shallow permafrost, for which appreciable thaw can take place during the interglacials of about 15,000 years. The equations and solution are discussed in Appendix B.

Syngenetic growth of permafrost

Syngenetic growth of permafrost occurs when material is deposited at the surface while freezing is in progress. This is inherently a much more efficient freeze process and the growth of frozen layers can be greatly accelerated. Figure 13 shows a sketch of the process with the surface deposit laid down such that the surface, held at a constant temperature T_s, is moving at a constant velocity U. The total frozen zone at any time is equal to the material frozen at the interface $X(t)$, plus the depositional layer U_t. The syngenetic system will be inherently unstable with no equilibrium solution. If the frozen zone should equal the heterogenetic steady-state value ($U = 0$), the motion of the upper surface will cause melting at the base of the permafrost.

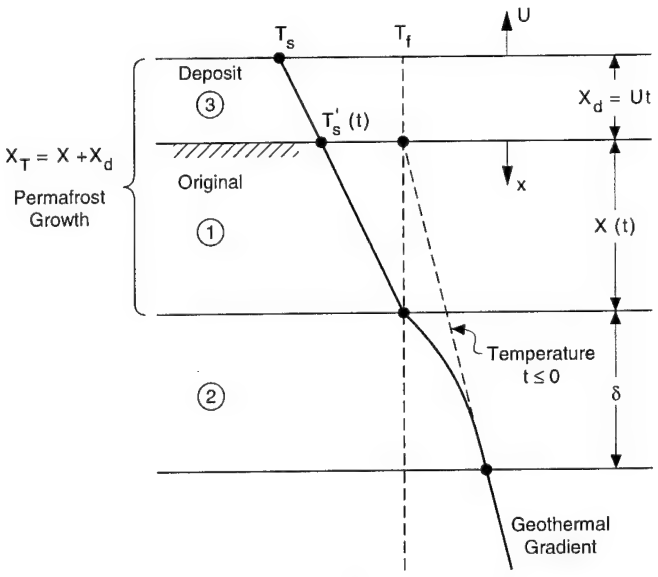

Figure 13. Geometry and coordinate system for freeze of a semi-infinite medium with moving upper surface.

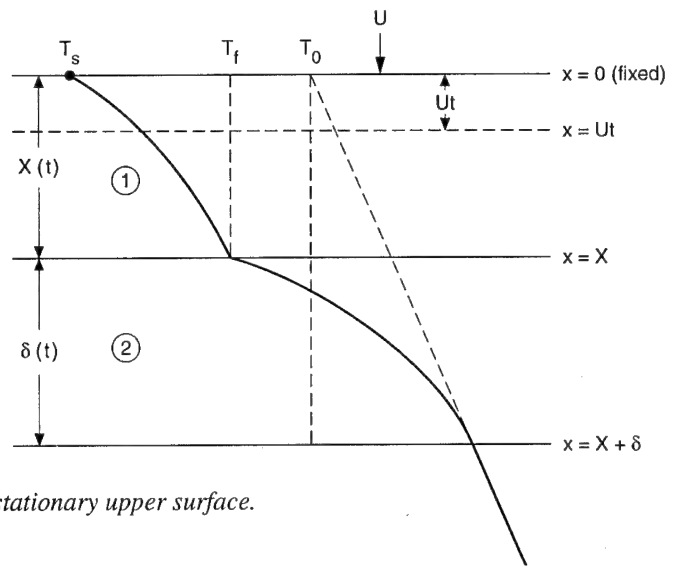

Figure 14. Coordinate system for stationary upper surface.

Thus, at some time during the formation process, the bottom must be melting to compensate for the depositional growth but the process cannot be steady.

Let us fix the upper surface so that it remains stationary, as shown in Figure 14. Then it would appear that a steady flow of material is moving at a constant velocity U and the original soil surface seems to be moving downward at a steady velocity. The energy equation is transformed such that a convective term exists. The equations for regions 1 and 2 are

$$\alpha_i \frac{\partial^2 T_i}{\partial x^2} - U\frac{\partial T_i}{\partial x} - \frac{\partial T_i}{\partial t} = 0 \qquad i = 1,2. \tag{25}$$

The boundary and initial conditions are exactly the same as those of the heterogenetic case (see Appendix C for details of the syngenetic equations).

The heat balance integral form of the energy equations is

$$\frac{d}{dt}\{\rho_1 c_1 \int_0^X T_1(x,t)dx + \rho_2 c_2 \int_X^{X+\delta} T_2(x,t)dx - \rho_1 \ell X + (\rho_2 c_2 - \rho_1 c_1)T_f X$$

$$-\rho_2 c_2 (X+\delta)\left[T_o + \frac{G}{2}(X+\delta)\right]\} = -k_1 \frac{\partial T_1(0,t)}{\partial x} + k_2 G - \rho_1 c_1 U \Delta T_1 - \rho_2 c_2 U\left[\Delta T + G(X+\delta)\right]. \tag{26}$$

We note that this is identical to the relation for heterogenetic growth, eq 5, except for the two additional terms on the right-hand side of eq 26. Carrying out the integrations and making eq 26 nondimensional, leads to the following result.

$$\tau = \int_0^\sigma K_1 d\sigma \tag{27}$$

$$K_1 = \frac{b_1 + b_2\beta - \frac{1}{6g}\left(1 - \frac{\sigma g'}{g}\right) - C_{21}\sigma\left(\frac{2}{3}\beta + 1\right) - \frac{C_{21}}{3}(\sigma + \phi)\sigma\beta'}{\frac{1}{\sigma}\left(\frac{1}{g} - 2\right) + k_{21} - \psi\left\{1 + 1/S_T + C_{21}\left[\phi + \sigma(\beta + 1)\right]\right\}} \tag{28}$$

where

$$\psi = \frac{U\Delta T_1}{G\alpha_1} .$$

Now the integration of eq 27 follows exactly as was done previously (see FORTRAN program PFTSYNB.FOR in Appendix E). The model requires only the ratios of the thawed to frozen values of thermal conductivity, specific heat capacity, and density for the permafrost soils, as was noted earlier.

Syngenetic model verification

It is possible to check the solution for a special case as was done for the heterogenetic growth. Although there is no exact solution for the phase-change case, there is an exact solution for the transient location of the T_f isotherm for the same problem with a homogeneous soil with zero latent heat, i.e, infinite Stefan number (Lunardini, in prep.). The relation is

$$e^{\psi\sigma_f}(B-1)\ \text{erfc}\frac{B}{2\sqrt{\tau}} - (A+1)\ \text{erfc}\frac{A}{2\sqrt{\tau}} + 2A = 0 \qquad (29)$$

where $A = \sigma_f - \psi\tau$

$B = \sigma_f + \psi\tau$

σ_f = location of T_f isotherm.

If we let the Stefan number be large and hold the property ratios to unity, the heat balance integral solution for syngenetic growth can be compared to this exact relation. Table 2 notes the results for typical cases.

Table 2. Movement of T_f isotherm, homogeneous soil, syngenetic freezing.
S_T =1000, $\ell = 0$, $T_f - T_s = 10°C$, $\phi = 0$, G = 0.0286°C/m.

τ	σ_f *exact*	σ_f *approximate*	*% difference*
	a. U = 10 mm/yr		
0.0014	0.0087	0.090	–1.5
0.0069	0.1634	0.1700	–4.0
2.033	0.7739	0.7700	0.5
2.8232	0.8206	0.8100	1.3
	b. U = 1 mm/yr		
0.005	0.1448	0.15	–3.6
0.099	0.3874	0.4006	–3.42
1.0689	0.6572	0.6662	–1.37
11.4705	0.8795	0.8720	0.85

The results indicate that the approximate technique gives excellent results, especially as the time increases. Thus, the Heat Balance Integral method and the numerical quadrature are robust even for very long time spans. See also eq C17 for further verification of the solution method with phase change.

DISCUSSION

Equation 9 was solved numerically using Simpson's rule. This resulted in values of the permafrost depth versus time as a function of S_T, ε and the thermal property ratios of the frozen and the thawed zones. The results are presented in Figures 15–17.

These graphs depend only upon the quantities S_T, ϕ and ε. In Appendix A it is shown that the soil porosity, ε, determines the saturated soil property ratios. The thermal property ratios used for the graphs are listed in Tables A1 and A2. The graphs are only valid for the particular soil ratios given. However, this does not affect the validity of the model itself. Any specific site can be modeled by using site-specific property ratios in eq 9. Figures 15–17 can be used to estimate permafrost formation times for a wide range of surface temperatures and geothermal gradients.

The graphs can also be applied to variable surface temperatures with a bit of manipulation. Figure 18

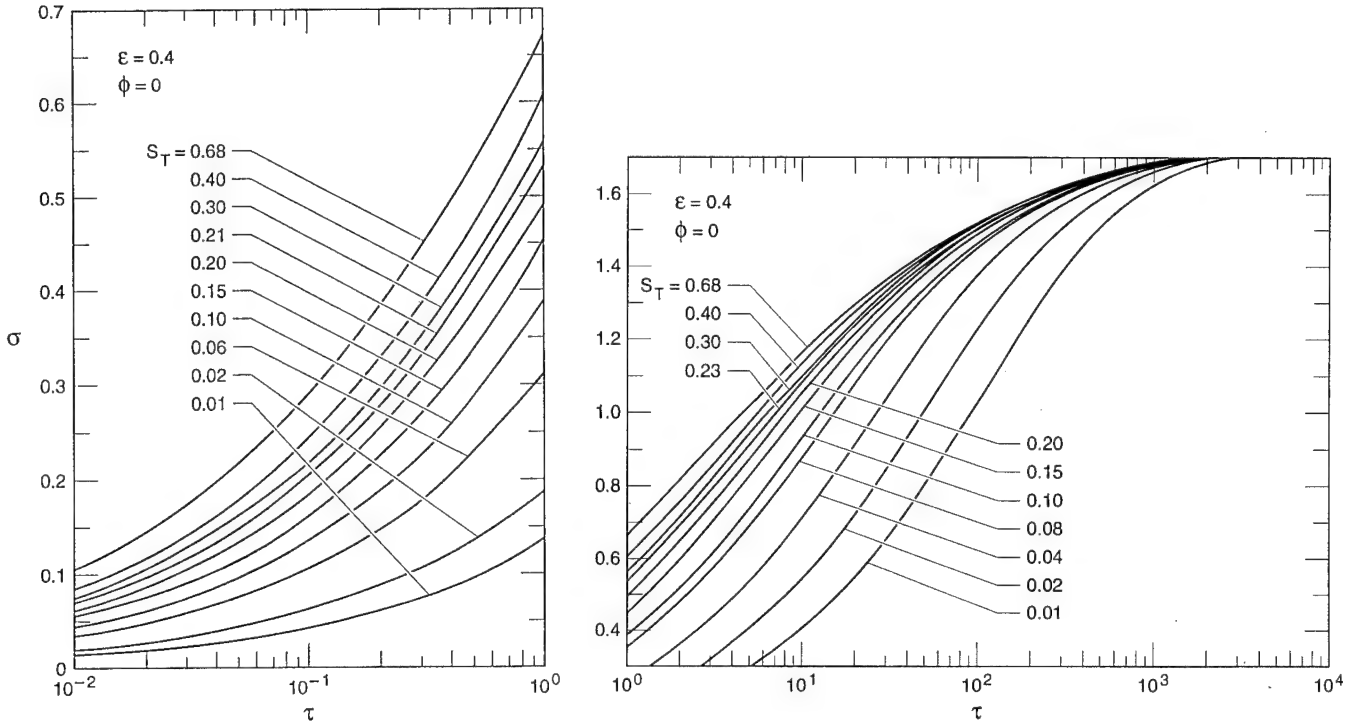

Figure 15. Formation time of permafrost, saturated mineral soils, ϕ = 0, ε = 0.4.

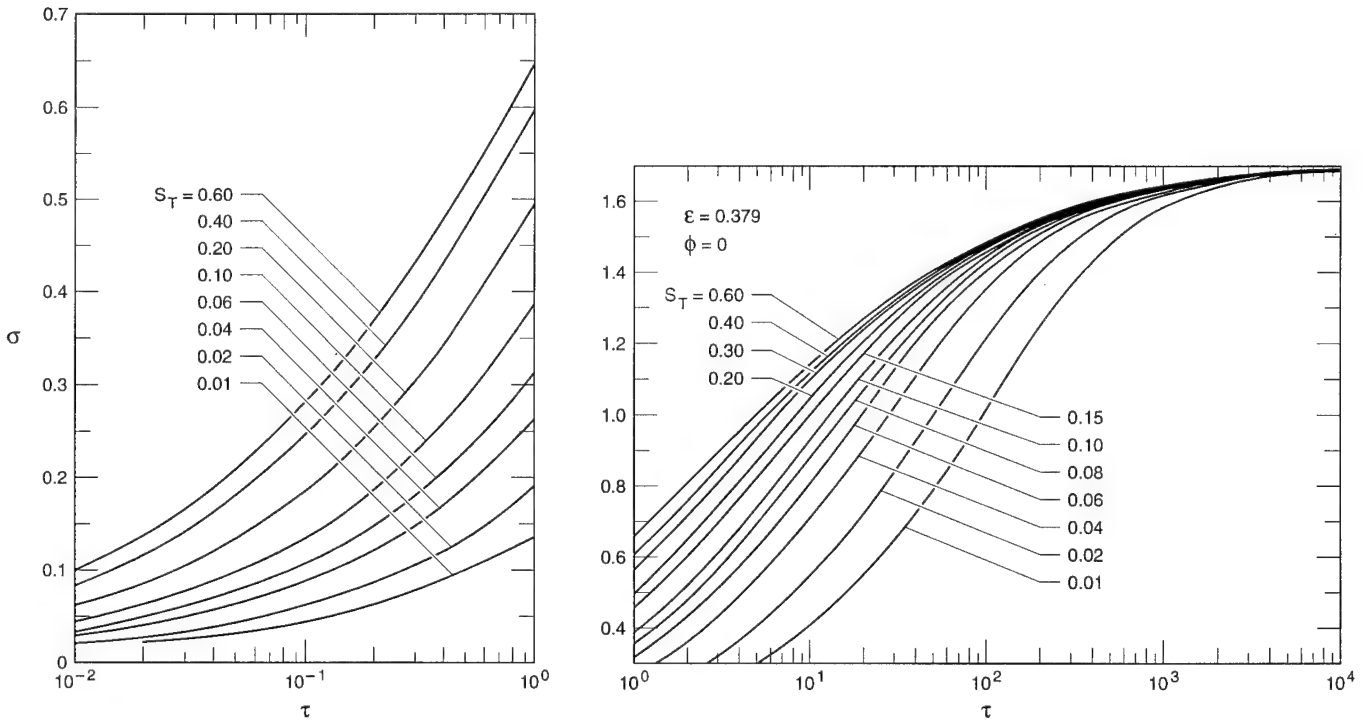

Figure 16. Formation time of permafrost, saturated mineral soils, ϕ = 0, ε = 0.379 (Prudhoe Bay, Alaska).

plots the time needed to reach 90% of the equilibrium permafrost thickness at a site. Figure 19 shows the thickness of permafrost formed after 15,000 years as a function of average surface temperature for different soils as characterized by the soil porosity. Figures 20 and 21 show that syngenetic growth greatly reduces the formation time during the latter stages of permafrost growth. However, there may be significant questions as to whether surface deposition has continued for long periods of time at any given location.

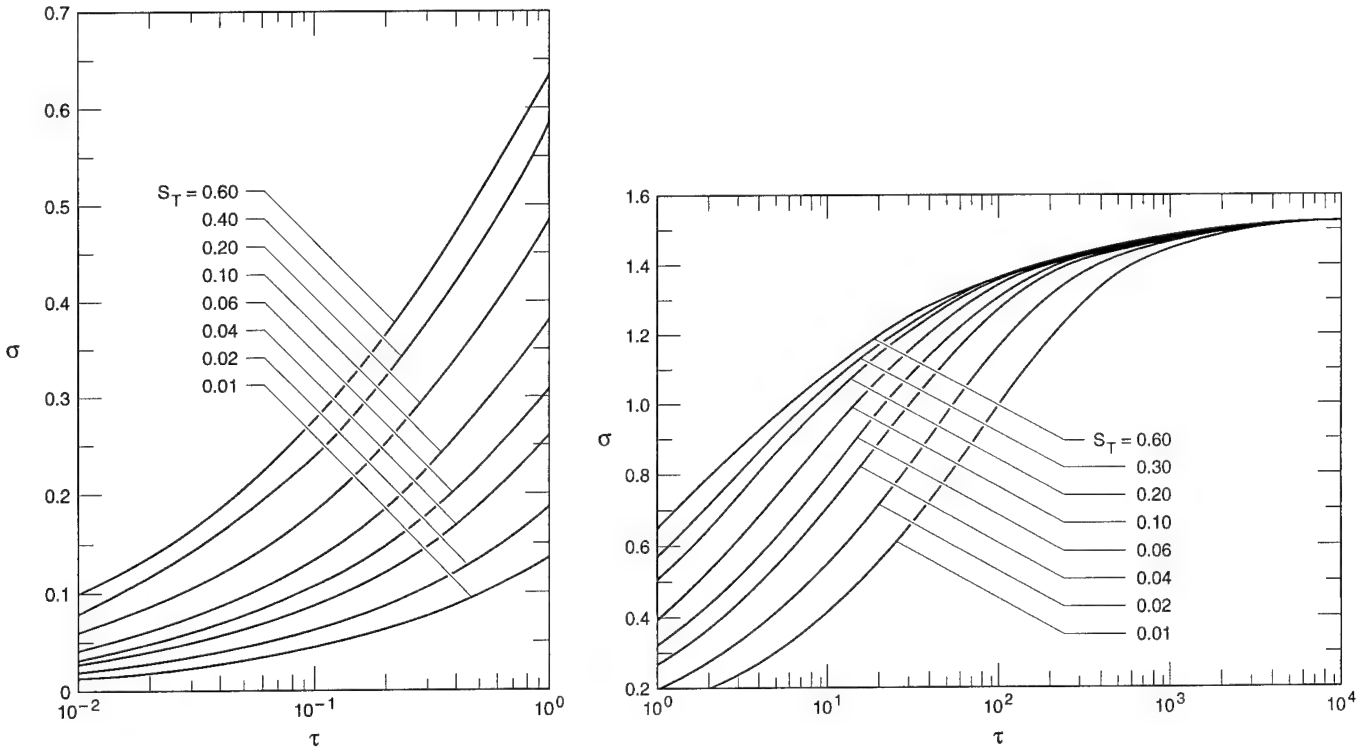

Figure 17. Formation time of permafrost, saturated mineral soils, ϕ = 0, ε = 0.3.

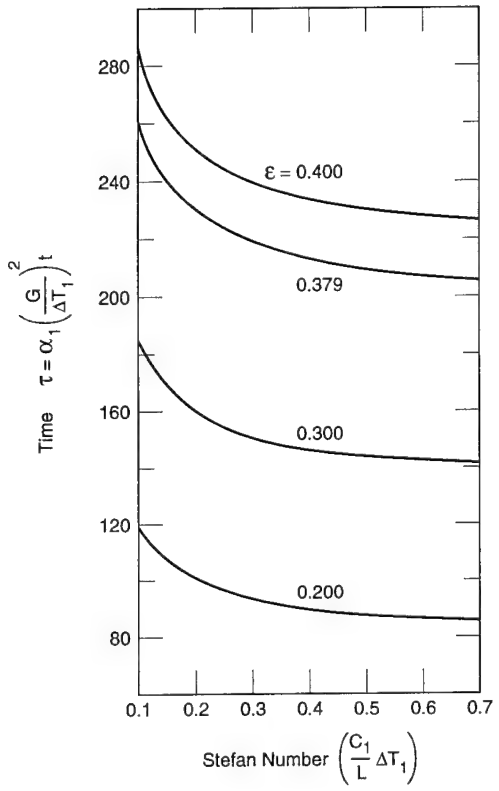

Figure 18. Formation time for permafrost to reach 90% equilibrium thickness, saturated mineral soils.

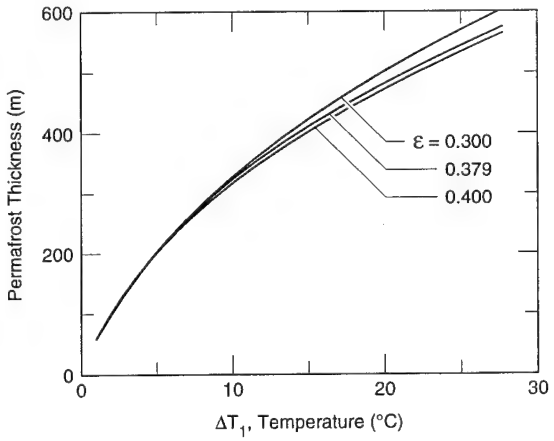

Figure 19. Effect of soil porosity on permafrost thickness after 15,000 years, saturated mineral soils, G = 0.0286°C/m.

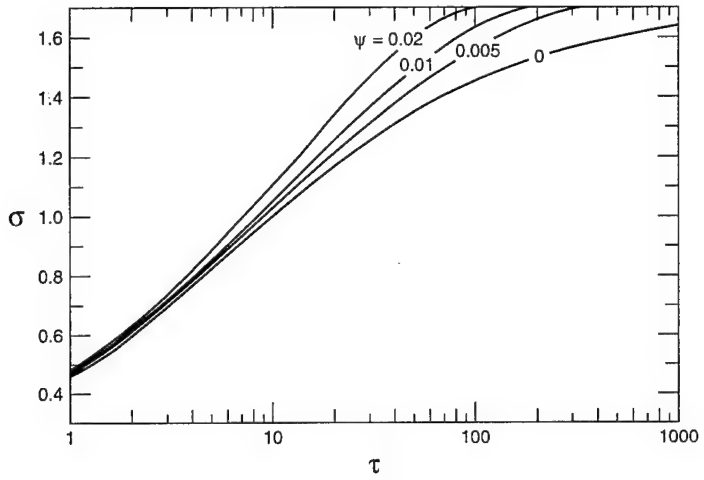

Figure 20. Syngenetic growth of permafrost, saturated mineral soils, $\phi = 0$, $\varepsilon = 0.379$, $S_T = 0.15$ (Prudhoe Bay, Alaska).

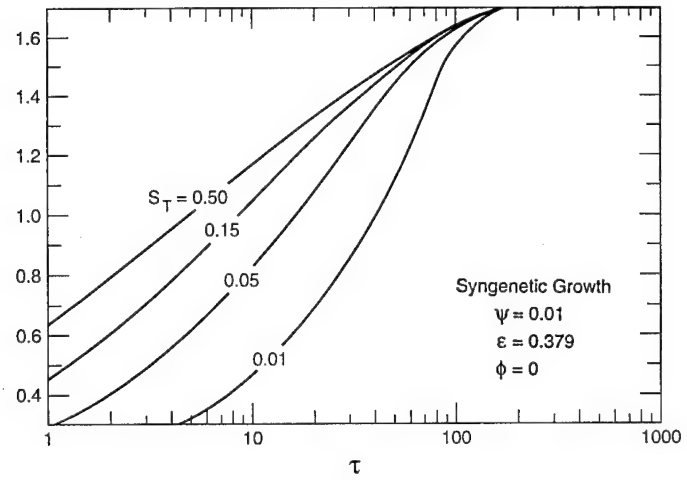

Figure 21. Syngenetic growth of permafrost, saturated mineral soils, $\phi = 0$, $\varepsilon = 0.379$, $\psi = 0.01$ (Prudhoe Bay, Alaska).

Table 3. Paleotemperature scenarios, Prudhoe Bay, Alaska (after Osterkamp and Gosink 1991).

Scenario	T_s* *(°C)*	*Duration before present time (years)*	*Stefan number*
Present (Lachenbruch et al. 1982)	−10.99	10,000–15,000	0.1438
Brigham and Miller (1983)	−13.69	240,000	0.1827
Matteucci (1989)	−11	300,000	0.1440
Vostok, Robin (1983)†	−16	160,000	0.2159
E. Siberia (Maximova and Romanovsky 1988)†	−11.3	170,000	0.1483

* Average value of the fluctuating surface temperature over the indicated time span.

† Fitted to present Prudhoe Bay surface temperature.

Prudhoe Bay, Alaska

Considerable information on the permafrost is available from oil wells in the Prudhoe Bay, Alaska, area (Lachenbruch et al. 1982). Using the actual permafrost data, we note that the property ratios for $\varepsilon = 0.379$ (Tables A1 and A2) are very close to measured and estimated values (Lachenbruch et al. 1982). Some temperature possibilities for Prudhoe are listed in Table 3. Figures 16a and b can be used to estimate the permafrost formation time, depending upon the temperature chosen.

Example 1

At Prudhoe Bay, Alaska, the permafrost has the following present conditions:

$$T_s = -10.99°C$$
$$G = 0.0286°C/m$$
$$\varepsilon = 0.379$$
$$S_T = 0.1440$$
$$\alpha_1 = 58.89\ m^2/yr$$
$$k_g = 4.34\ W/m\ K$$
$$\text{measured } k_{21} = 0.5795$$
$$\text{measured present permafrost thickness, } X_p = 599.3\ m.$$

Then, the equilibrium permafrost thickness is

$$X_e = \frac{\Delta T_1}{k_{21} G} = 602.8\ m.$$

The calculated equilibrium thickness is essentially the same as the measured value. How long would it take to reach this depth if the surface temperature had been $T_s = -10.99°C$ for an indefinite period? The nature of the solution is such that the final equilibrium values will be reached only after very long times. From Figure 18 we find the time to reach 90% of equilibrium (542.0 m) is

$$\tau = \alpha_1 \left(\frac{G}{\Delta T_1} \right)^2 t = 241.2$$

thus $t = 500{,}740$ years. This time is obviously quite long and suggests that the present climate of Prudhoe Bay is probably considerably warmer than it has been on average over the past glacial cycles. Such warming over the past 15,000 years is widely accepted.

Example 2

Prudhoe Bay, with the Brigham and Miller (1983) paleotemperature scenario, has the following: $T_s = -13.69°C$ for 225,000 years before warming to $-11°C$ in the last 15,000 years. For this case $X_e = 763.5$ m. For $t = 225{,}000$ years, $\tau = 67.3$. From Figure 16, with $S_T = 0.1827$, we read $\sigma = 1.412$. Thus, in 225,000 years the permafrost will grow to $X = 626.5$ m. This value will then slowly decay to the new equilibrium of 602.8 m over 15,000 years. This requires a melt rate of 1.58 mm/yr. This value is well within the estimated average thaw rate of 2.5 mm/year for this case (see Appendix D). Note that a lower surface temperature will greatly accelerate growth since the new equilibrium depth will be greater than before. Hence, a much larger fraction of the growth will be during the early, rapid growth stage.

Figure 22 shows the permafrost thickness at Prudhoe Bay after six glacial cycles with some typical features of permafrost growth demonstrated. First, the initial permafrost growth is quite rapid, reaching a thickness of 570 m after 120,000 years, with the paleotemperature model of Figure 7a. The thickness then slowly approaches an equilibrium value of 739 m but it will surpass the present thickness of 600 m after about 185,000 years. Thus, a paleotemperature model as cold as that of Figure 7b will yield permafrost that is too thick. Also shown is the finite difference prediction of Osterkamp and Gosink (1991), using Figure 6 (which has the same mean temperature as Fig. 7a) and starting with 600 m of permafrost, that indicates much faster permafrost growth and thicker permafrost. Their quasi-steady model neglects sensible heat, as-

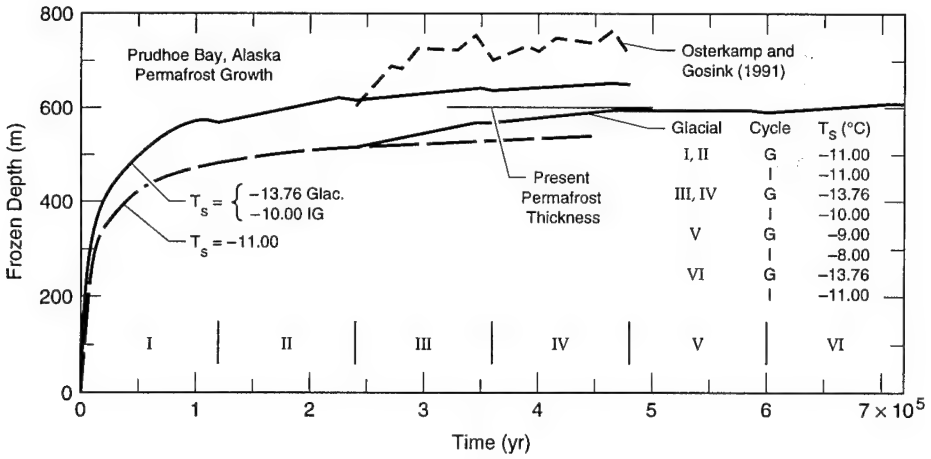

Figure 22. Growth of permafrost at Prudoe Bay, Alaska; effect of paleotemperature scenarios.

sumes fixed geothermal heat flow to the freezing interface, and starts with permafrost depth far less than equilibrium. All of these approximations overestimate the freeze rate. The second curve of Figure 22 shows the significant effects if the paleotemperature model is modified by only a small amount. The predicted permafrost thickness will reach present values after about 640,000 years and will tend to oscillate about this value.

Table 4. Effect of previous cooling on permafrost growth time.* X = 541.0 m.

Case	G	*Time (years)*	*Comment*
No pre-cool	0.0286	486,100	uses eq 10
Pre-cool	0.0220	78,900	uses eq 10
Pre-cool	0.0286	105,400	uses eq B15
Syngenetic	0.0286	172,500	eq 27, U = 1 mm/yr

* Soil properties for Prudhoe Bay, ΔT_1 = 10.0°C.

Example 3

Consider the effect of previous cooling at Prudhoe Bay. If the equivalent geothermal gradient is G = 0.0220°C, then the time to reach 541 m is 78,940 years. The results of three possibilities are shown in Table 4. Note the very large effect of previous cooling or cyclic thermal modulation.

Table 5. Formation time of deep permafrost.* X_e = 1813 m.

Case	G	*Time (years)*	*Comment*
No pre-cool	0.0286	4,190,600	uses eq 10
Pre-cool	0.0220	488,900	uses eq 10
Pre-cool	0.0286	358,900	uses eq B15
Syngenetic	0.0286	784,100	eq 27, U = 1mm/yr
Neumann (ϕ = 0)	0.0	64,800	absolute minimum time

* Soil properties for Prudhoe Bay, ΔT_1 = 29.3°C.

Deep permafrost

Example 1

Consider the case of very thick permafrost, on the order of 1600 m. Let the properties be those of Prudhoe Bay but ε = 0.4, ΔT_1 = 29.27°C, G = 0.0286, α_1 = 57.99 m^2/yr, then X_e =1813 m. The value of the surface temperature chosen is on the order of 12°C less than present winter temperatures experienced in parts of Canada, Russia and Greenland, although it is doubtful that such temperatures could have persisted for 1 million years. The value used illustrates the long time needed to form deep permafrost by conduction alone. We will find the time required to form 90% of the permafrost or 1632 m. The calculations are as before, with S_T = 0.4 (see Fig. 15 for the case without previous cooling). The results are given in Table 5. The formation time is very long, even with previous cooling. This example used Prudhoe Bay properties and geothermal gradient, which could be significantly different at a site in Siberia with deep permafrost.

Example 2

Consider the question of the maximum permafrost thickness that is probable. This will occur if the frozen thermal conductivity is large, the geothermal heat flow and latent heat are low, and the surface temperature is minimal (within the constraints discussed earlier). Let ε = 0.2, T_s = –23.5°C, q_g = 0.042 W/m^2, and assume coarse-grained soil with k_g = 5.86 W/m K. The results of the calculation are shown in Table 6.

The permafrost reaches a thickness of 2132 m after 1 million years and a value of 2255 m after 2 million years. Balobaev et al. (1978) note that the greatest permafrost thicknesses recorded are on the East Siberian platform and present graphs with maximum permafrost thicknesses of 1500 m. These thicknesses are on the order of the value predicted here and it is not likely permafrost much thicker than this has ever existed, since the required time exceeds the plausible time available. These extreme thicknesses are not in thermal equilibrium with the present surface temperatures and are slowly thawing.

Table 6. Extreme predicted permafrost thickness.

Time (years)	X *(m) heterogenetic*	X *(m) syngenetic* U = *1 mm/yr*
100,000	1488.4	1539.9
532,257	2000.0	2158.6
1,000,000	2132.0	2362.9
2,000,000	2254.5	2529.5
Infinity	2600.2	2600.2

CONCLUSIONS

The calculations and examples indicate that the growth of permafrost, with pure conduction heat transfer, is governed by the transient surface temperature, the geothermal heat flow and the soil thermal properties. Permafrost grows very rapidly for an initial phase and then asymptotically approaches a steady-state value after time spans of immense length. Very thick permafrost may have required the total Quaternary Period to form. It is likely that permafrost is not in equilibrium at most sites. The bottom growth and decay of permafrost are so slow that accurate methods of detecting which is occurring (or if equilibrium exists) are not available for the field. Permafrost less than 600 m can grow within 50,000 years, with surface temperatures only slightly lower than present values, but deeper permafrost depths require time scales of several ice ages and quite low temperatures to form.

LITERATURE CITED

Allen, D., F. Michel and A. Judge (1988) Paleoclimate and permafrost in the Mackenzie Delta. In *Proceedings, 5th International Conference on Permafrost, 2–5 August, Trondheim, Norway.* Trondheim, Norway: Tapir Publishers, vol. 1, p. 33–38.

Balobaev, V.T., V.N. Devyatkin and I.M. Kutasov (1978) Contemporary geothermal conditions of the existence and development of permafrost. In *Permafrost: The North American Contribution to the 2nd International Conference on Permafrost, 13–28 July, Yakutsk.* Washington, D.C.: National Academy of Sciences, p. 8–12.

Brigham, J.K. and G.H. Miller (1983) Paleotemperature estimates of the Alaskan Arctic Coastal Plain during the last 125,000 years. In *Proceedings, 4th International Conference on Permafrost, 17–22 July, Fairbanks, Alaska.* Washington, D.C.: National Academy Press, p. 80–85.

Brown, R.J.E. (1964) Permafrost investigations on the Mackenzie Highway in Alberta and Mackenzie District. Ottawa, Canada: National Research Council, NRC 7885.

Bryan, K. (1946) Cryopedology—The study of frozen ground and intensive frost action with suggestions on nomenclature. *American Journal of Science,* **244**: 622–642.

Carslaw, H.S. and C.J. Jaeger (1959) *Conduction of Heat in Solids,* 2nd edition. Oxford: Clarendon Press.

COHMAP Members (1988) Climatic changes of the last 18,000 Years: Observations and model simulations. *Science*, **241**: 1043–1052.

Dansgaard, W. and H. Oeschger (1989) Past environmental long-term records from the Arctic. In *The Environmental Record in Glaciers and Ice Sheets* (H. Oeschger and C.C. Langway, Jr., Ed). New York: John Wiley and Sons, p. 288–317.

Eddy, J.A. and R.S. Bradley (1991) Changes in time of the temperature of the earth. *EarthQuest*, **5**(1).

Folland, C.K., T.R. Karl and K.YA. Vinnikov (1990) Observed climate variations and change. In *Climate Change, The IPCC Scientific Assessment*, chapter 7 (J.T. Houghton, G.J. Jenkins and J.J.Ephraums, Ed.). Cambridge: Cambridge University Press.

Gold, L.W. and A.H. Lachenbruch (1973) Thermal conditions in permafrost—A review of North America literature. In *Permafrost: The North American Contribution to the 2nd International Conference on Permafrost, 13–28 July, Yakutsk.* Washington, D.C.: National Academy of Sciences, p. 3–25.

Goodman, T.R. (1958) The heat-balance integral and its application to problems involving a change of phase. *ASME Transactions,* **80**: 335–342.

Jouzel, J., C. Lorius, J.R. Petit, C. Genthon, N.I. Barkov, V.M. Kotlyakov and V.N. Petrov (1987) Vostok ice core: A continuous isotope temperature record over the last climatic cycle (160,000 years). *Nature*, **329**: 403–408.

Katasonov, E.M. (1988) Continuous persistence of the permafrost zone during the Quaternary Period. In *Proceedings, 5th International Conference on Permafrost, 2–5 August, Trondheim, Norway.* Trondheim, Norway: Tapir Publishers, vol. 1, p. 801–804.

Kersten, M.S. (1949) Thermal properties of soils. University of Minnesota Experimental Station, Bulletin no. 28.

Lachenbruch, A.H., J.H. Sass, B.V. Marshall and T.H. Moses, Jr. (1982) Permafrost, heat flow and the geothermal regime at Prudhoe Bay, Alaska. *Journal of Geophysical Research,* **87**(B11): 9301–9316.

Lozano, C.J. and R. Reemsten (1981) On a Stefan problem with an emerging free boundary. *Numerical Heat Transfer*, **4**: 39–245.

Lunardini, V.J. (1980) Phase change around a circular pipe. USA Cold Regions Research and Engineering Laboratory, CRREL Report 80–27.

Lunardini, V.J. (1981a) *Heat Transfer in Cold Climates*. New York: Van Nostrand Reinhold.

Lunardini, V.J. (1981b) Application of the heat balance integral to conduction phase change problems. USA Cold Regions Research and Engineering Laboratory, CRREL Report 81–25.

Lunardini, V.J. (1982) Freezing of soil with surface convection. In *Proceedings, 3rd International Symposium on Ground Freezing, 22–24 June, Hanover, N.H.* USA Cold Regions Research and Engineering Laboratory, p. 205–213.

Lunardini, V.J. (1984) Freezing of a semi-infinite medium with initial temperature gradient. *Journal of Energy Resources Technology,* **106**: 103–106.

Lunardini, V.J. (1991) *Heat Transfer With Freezing and Thawing*. Amsterdam: Elsevier (Amsterdam, Oxford, New York, Tokyo).

Lunardini, V.J. (in prep.) Permafrost and ground temperature calculations. USA Cold Regions Research and Engineering Laboratory Report.

Lunardini, V.J. and R. Varotta (1981) Approximate solution to Neumann problem for soils systems. *ASME Journal of Energy Resources Technology*, **103**(1): 76–81.

Matteucci, G. (1989) Orbital forcing in a stochastic resonance model of the late-Pleistocene climatic variations. *Climate Dynamics,* **3**: 179–190.

Maximova, L.N. and V.Y. Romanovsky (1988) A hypothesis for the Holocene permafrost evolution. In *Proceedings, 5th International Conference on Permafrost, 2–5 August, Trondheim, Norway.* Trondheim, Norway: Tapir Publishers, vol. 1, p. 102–106.

Muller, S.W. (1945) Permafrost or permanently frozen ground and related engineering problems. Special Report, Strategic Engineering Study No. 62, U.S. Army Engineers, Military Intelligence Division Office.

Neumann, F. (c. 1860) Lectures given in 1860s, cf. Reimann-Weber, Die partiellen Differentialgleichungen. *Physik*, Edition 5, vol. 2, 1912, p. 121.

Osterkamp, T.E. and J.P. Gosink (1991) Variations in permafrost thickness in response to changes in paleoclimate. *Journal of Geophysical Research*, **96**(B3): 4423–4434.

Robin, G. de Q. (1983) *The Climate Record in Polar Ice Sheets.* New York: Cambridge University Press.

Romanovsky, N.N., V.N. Zaitsev, S.Yu. Volchenkoc, V.P. Volkova and O.M. Lisitsina (1988) New data on permafrost of Kodar-Chara-Udokan Region. In *Proceedings, 5th International Conference on Permafrost, 2–5 August, Trondheim, Norway.* Trondheim, Norway: Tapir Publishers, vol. 1, p. 233–236.

Schlichting, H. (1968) *Boundary Layer Theory*, 6th edition. New York: McGraw-Hill Book Co.

Sun, Jianzhong and Li, Xinguo (1988) Division and temperature condition of the last glaciation in northern China. In *Proceedings, 5th International Conference on Permafrost, 2–5 August, Trondheim, Norway.* Trondheim, Norway: Tapir Publishers, vol. 1, p. 107–112.

Swinzow, G.K. (1969) Certain aspects of engineering geology in permafrost. *Journal of Engineering Geology,* **3**: 177–215.

Tao, L.N. (1978) The Stefan problem with arbitrary initial and boundary conditions. *Quarterly of Applied Mathematics,* **36**(3): 223–233.

Yuen, W.W. (1980) Application of the heat balance integral to melting problems with initial subcooling. *International Journal of Heat and Mass Transfer*, **23**: 1157–1160.

APPENDIX A: SOIL PROPERTIES AND RATIOS

The thermal conductivity of a mixture such as a soil can be estimated by using the weighted geometric mean (Lachenbruch et al. 1982, Gold and Lachenbruch 1973, Lunardini 1981a). This can be written for a general soil as

$$k = \left(k_g\right)^{x_g} \left(k_w\right)^{x_w} \left(k_a\right)^{x_a} \left(k_i\right)^{x_i} \tag{A1}$$

where k_a, k_g, k_i and k_w are the thermal conductivities of air, soil solids, ice and water; x_a, x_g, x_w and x_w are the volumetric fractions of air, soil solids, ice and water. The geometric mean is usually better than the assumption of parallel geometry (weighted arithmetic mean), which is often used for simplicity.

Saturated soil

Many assumptions can be made concerning the soil saturation and porosity but simple approximations will be used here. If the soil is always saturated, has a constant void ratio ε, and all of the water freezes, then $x_w = \varepsilon$ and the conductivity ratio can be expressed as

$$k_u = k_w^{\varepsilon}\left(\gamma k_g\right)^{(1-\varepsilon)} \tag{A2}$$

$$k_f = k_i^{\varepsilon}\left(k_g\right)^{(1-\varepsilon)} \tag{A3}$$

$$k_u / k_f = k_{21} = \left(k_w / k_i\right)^{\varepsilon\gamma(1-\varepsilon)} \tag{A4}$$

where $\gamma = 0.9825$ is a temperature correction for k_g (Lachenbruch et al. 1982) and $k_w/k_i = 1.34/5.45 = 0.2459$.

The volumetric specific heat for the system may be expressed as follows, for the thawed and frozen states

$$C_u = C_{su}\,(1 - x_w) + C_w\,x_w \tag{A5}$$

$$C_f = C_{sf}\,(1 - x_i) + C_i\,x_i \tag{A6}$$

where C_{su} and C_{sf} are the volumetric specific heats of unfrozen and frozen solids, and C_w and C_i are the volumetric specific heats of water and ice.

It is fortunate that the volumetric specific heats of soil solids and ice are all about the same. For example, the specific heat of organic solids is 0.461 cal/cm^3 °C, for mineral solids it is 0.420, and for ice it is 0.459 (Lunardini 1981a). If one assumes that the values for the solids, except for ice, change little through the phase change then

$$C_f = 0.4202 + 0.0388\varepsilon \tag{A7}$$

$$\frac{C_u}{C_f} = C_{21} = \frac{0.4296 + 0.5708\varepsilon}{0.4202 + 0.0388\varepsilon}. \tag{A8}$$

The density ratio is

$$\frac{\rho_u}{\rho_f} = \rho_{21} = \frac{1 - 0.6154\varepsilon}{1 - 0.650\varepsilon}. \tag{A9}$$

Finally, the ratio of thermal diffusivities is

$$\frac{\alpha_u}{\alpha_f} = \alpha_{21} = \frac{k_{21}}{C_{21}}. \tag{A10}$$

The latent heat is

$$L = 79.71\ \varepsilon \tag{A11}$$

The Stefan Number is

$$S_T = \frac{C_l}{\ell}(T_l - T_s) = \frac{C_l \Delta T_l}{L} = \frac{0.4202 + 0.0388\varepsilon}{79.71\varepsilon}\Delta T_l. \tag{A12}$$

It is possible to present the results for soil systems, quite efficiently, since the property ratios can be described as functions of the soil void ratio ε (Lunardini and Varotta 1981). Using the thermal conductivities of Table A1, the property ratios used in the calculations are given in Table A2. The thermal conductivity ratio will be representative of soil that is not too dry. Thus, eq A4 and A10 should be acceptable if $\varepsilon \geq 0.2$ (Kersten 1949).

Table A1. Thermal conductivity of materials.

Substance	*Thermal conductivity W/(m°C)*
Water	0.561
ice	2.281
air	0.0237
silicaceous soil solids*	4.29–5.87

*Lachenbruch et al. (1982)

Table A2. Calculated saturated granular soil thaw–freeze property ratios.

Soil porosity ε	k_u/k_f *eq 21*	C_u/C_f *eq 24*	α_u/α_f *eq 26*	ρ_u/ρ_f *eq 25*
0.2	0.7448	1.2706	0.5862	1.008
0.3	0.6484	1.3909	0.4662	1.0129
0.379	0.5812	1.4847	0.3915	1.0174
0.4	0.5645	1.5094	0.3740	1.0187
0.5	0.4915	1.6265	0.3022	1.0256

Balobaev et al. (1978) note that for limestone and dolomite, $k = 2.44 - 3.37$ W/m °C and $q_g = 0.017 - 0.021$ W/m^2 at 60–800 m, anomalously low heat flow values.

Nonsaturated soil

For the nonsaturated soil, assuming that the porosity does not change during phase changes, the ratio of thawed to frozen thermal conductivity

$$k_u = \left(\gamma k_g\right)^{(1-\varepsilon)} k_w^{\varepsilon S} k_a^{(1-S)} \tag{A13}$$

$$k_f = \left(k_g\right)^{(1-\varepsilon)} k_i^{\varepsilon S \rho_{wi}} k_a^{\varepsilon(1-S\rho_{wi})} \tag{A14}$$

$$\frac{k_u}{k_f} = \gamma^{(1-\varepsilon)}\left[k_w / \left(k_i\right)^{\rho_{wi}}\right]^{\varepsilon S} k_a^{\varepsilon S(\rho_{wi}-1)} \tag{A15}$$

where S is the thawed soil saturation level, $\rho_{wi} = \rho_w / \rho_i$; $\rho_i/\rho_w = 0.91$. Interestingly, the ratio k_{21} can have the same values as for the saturated case if the saturation has certain values, e.g., $S = 0.756$, $\varepsilon = 0.379$.

APPENDIX B: QUATERNARY CYCLIC THERMAL MODULATION

Thaw process

Assuming that melting occurs with a fraction f of the geothermal heat flow going into increasing the sensible heat allows an estimate to be made of the thaw time and the final temperature, noted in Figure 12, which will then be the initial temperature distribution for the next freeze cycle. Referring to Figure 11, we assume that the fraction of geothermal energy available for melt at any time is

$$f = \frac{(f_m - 1)X + X_o}{X_o} \tag{B1}$$

where f_m is the melt fraction at the conclusion of melt and X_o is the initial frozen thickness. The temperature in the region of changing temperature is

$$T_2 = T_f + b(x - \Delta_1) + c(x - \Delta_1)^2 \tag{B2}$$

where $\Delta_1 = X_o - X$ and b,c are functions of time only. The initial temperature of the soil is

$$T_i = \begin{cases} T_f & x \le X_o \\ T_f + G(x - X_o) & x \ge X_o \end{cases}. \tag{B3}$$

The sensible heat added to the soil is

$$Q_s = C_u \int_{X_o - X}^{X_o} (T_2 - T_i)dx + C_u \int_{X_o}^{X_o + \delta} (T_2 - T_i)dx. \tag{B4}$$

The sensible heat addition is shown as the shaded region of Figure B1. The sensible heat at any instant is then

$$Q_s = \frac{1}{3} G C_u X\left(\delta - \frac{X}{2}\right). \tag{B5}$$

The change in sensible heat must equal the fraction of the geothermal energy not used for melting, or

$$\frac{dQ_S}{dt} = q_g(1 - f). \tag{B6}$$

The energy balance at the melt interface is

$$L\frac{dX}{dt} = fq_g. \tag{B7}$$

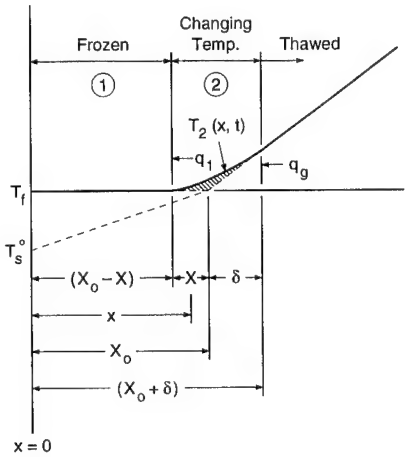

Figure B1. Bottom melt process.

The solutions to these equations lead to

$$\frac{1}{3} G C_u X\left(\delta - \frac{X}{2}\right) = q_g\left[t + \frac{1}{M}\left(1 - e^{Mt}\right)\right] \tag{B8}$$

$$X = \frac{X_o\left(1 - e^{Mt}\right)}{(1 - f_m)} \tag{B9}$$

where

$$M = \frac{(f_m - 1)q_g}{X_o L}.$$

The time to complete melt is

$$t_m = \frac{X_o L \ln f_m}{q_g (f_m - 1)}. \tag{B10}$$

This leads to the value of δ when melt is completed.

$$\delta_o = \frac{X_o}{2} + \frac{3L}{GC_u}\left(\frac{\ln f_m}{f_m - 1} - 1\right). \tag{B11}$$

We define a linear temperature distribution that will have the same sensible heat when thaw is completed.

$$T_i' = T_f + G'x \tag{B12}$$

$$\frac{G'}{G} = \frac{\delta_o - \frac{X_o}{3}}{\delta_o + X_o}. \tag{B13}$$

where G' is the equivalent geothermal gradient. Finally, the new temperature distribution at the beginning of freeze is

$$T_i = T_f + b_o x + c_o x^2 \tag{B14}$$

where

$$b_o = \frac{G(\delta_o - X_o)}{\delta_o + X_o}, \quad c_o = \frac{GX_o}{(\delta_o + X_o)^2}.$$

This initial temperature distribution is shown as curve a in Figure 12. Table B1 shows some results for Prudhoe Bay. Note the long melt times even if f is as high as 90%.

Table B1. Melt relations for Prudhoe Bay.

f_m	$\tilde{f}$	$\frac{\ln f_m}{f_m - 1} - 1$	δ_o (m)	$\frac{G'}{G}$	Melt time (years)
0.1	0.55	1.5584	7948.1	0.9064	108,926
0.2	0.60	1.0118	5265.6	0.8636	85,654
0.3	0.65	0.720	3833.5	0.8196	73,230
0.4	0.70	0.5272	2887.3	0.7706	65,022
0.5	0.75	0.3863	2195.8	0.7139	59,023
0.6	0.80	0.2771	1659.9	0.646	54,373
0.8	0.90	0.1157	867.8	0.455	47,502

X_o = 600 m, L = 30.21 cal/cm^3, C_u = 0.6457 cal/cm^3 °C.
$q_g = 1.35 \times 10^{-6}$ cal/cm^2 s, G = 0.0286°C.

Freeze of cooled soil

The freezing process is as discussed earlier except that the initial soil temperature is lowered as noted in Figure 10. The basic equations used earlier are still valid except that the coefficients of eq 6 and 7 change, owing to the new initial temperature given by eq B14. The basic equation, replacing eq 9, is

$$\frac{dF\sigma}{d\tau} = k_{21} - \frac{1}{\sigma}\left(2 - \frac{1}{g}\right) \tag{B15}$$

$$F = -\left(\frac{1}{6g} + \frac{1}{3} + \frac{\rho_{21}}{S_T}\right) - C_{21}\sigma\left[\frac{\beta^2}{6} - m_o\left(\frac{\beta^2}{6} - \frac{\beta}{3} - \frac{1}{2}\right) - \frac{\sigma S_o}{3}(\beta - 1)(\beta + 1)^2\right] \tag{B16}$$

$$\frac{\beta}{g} - k_{21}\sigma\left[-\beta + 2m_o(\beta + 1) + 2\sigma S_o(\beta + 1)^2\right] = \frac{2\rho_{21}(g - 1)\beta}{S_T} \tag{B17}$$

$$g = 1 - \frac{\alpha_{21}(Q-\beta)}{\beta(2Q-\beta)} \tag{B18}$$

where $Q = m_0\,(\beta+1) + \sigma S_o\,(\beta+1)^2$

$m_0 = b_0/G$

$S_0 = c_0 \Delta T_1 / G^2$.

The solution to these equations follows in exactly the same way as previously discussed.

APPENDIX C: HEAT BALANCE INTEGRAL EQUATIONS FOR SYNGENETIC PERMAFROST GROWTH

Method 1

We will formulate the basic equations in terms of a convective system with mass flowing through the stationary upper surface at constant velocity U, as shown in Figure 14. The governing equations are

$$\alpha_1 \frac{\partial^2 T_1}{\partial x^2} - U\frac{\partial T_1}{\partial x} - \frac{\partial T_1}{\partial t} = 0 \qquad 0 \le x \le X \tag{C1}$$

$$T_1(X,t) = T_f \tag{C1a}$$

$$T_1(0,t) = T_s \tag{C1b}$$

$$\alpha_2 \frac{\partial^2 T_2}{\partial x^2} - U\frac{\partial T_2}{\partial x} - \frac{\partial T_2}{\partial t} = 0 \qquad X \le x \le X+\delta \tag{C2}$$

$$T_2(X,t) = T_f \tag{C2a}$$

$$\frac{\partial T_2(X+\delta,t)}{\partial x} = G \tag{C2b}$$

$$T_2(X+\delta,t) = (X+\delta)G + T_o. \tag{C2c}$$

The initial temperature at the beginning of freeze is

$$T_i = T_o + Gx. \tag{C2d}$$

The energy balance at the phase change interface for the freeze process is

$$k_1 \frac{\partial T_1}{\partial x}(X,t) - k_2 \frac{\partial T_2}{\partial x}(X,t) + \rho_2 \ell U = \rho_2 \ell \frac{dX}{dt}. \tag{C3}$$

Because of the initial temperature distribution, during freeze, the heat flow to the interface from the thawed region will exceed the geothermal heat flow until equilibrium is established. Likewise, during a thaw period, the heat flow from the thawed zone will be less than the deep geothermal heat flow. The energy balance at the freezing front can also be written as two equations (Lunardini 1981b)

$$-k_1\left[\frac{\partial T_1(X,t)}{\partial x}\right]^2 + k_2 \frac{\partial T_2(X,t)}{\partial x}\frac{\partial T_1(X,t)}{\partial x} = \rho_1 \ell \alpha_1 \frac{\partial^2 T_1(X,t)}{\partial x^2} \tag{C4}$$

$$-k_1 \frac{\partial T_1(X,t)}{\partial x}\frac{\partial T_2(X,t)}{\partial x} + k_2\left[\frac{\partial T_2(X,t)}{\partial x}\right]^2 = \rho_2 \ell \alpha_2 \frac{\partial^2 T_2(X,t)}{\partial x^2}. \tag{C5}$$

Quadratic temperature profiles in regions 1 and 2 that satisfy the boundary conditions are

$$T_1 = T_f + a_1 X\left(\frac{x-X}{X}\right) + (a_1 X - \Delta T_1)\left(\frac{x-X}{X}\right)^2 \tag{C6}$$

$$T_2 = T_f + \left[G(\delta + 2X) + 2\Delta T\right]\left(\frac{x - X}{\delta}\right) - (GX + \Delta T)\frac{(x - X)^2}{\delta^2} \tag{C7}$$

where

$$a_1 X = \frac{\Delta T_1}{g}, \qquad g = \frac{\alpha_{21}(\Delta T + GX)X}{\delta\left[G(\delta + 2X) + 2\Delta T\right]} + 1.$$

In general, the simplest temperature profiles that will satisfy the boundary conditions should be chosen. The accuracy of the method increases as the order of a polynomial temperature choice increases; however, the use of high-order polynomials (third and higher) is often not justified since a small increase in accuracy requires significantly more computational effort. Equation C5 can be used to find a relation between X and δ. In nondimensional form this is

$$\frac{\beta}{g} - k_{21}\left[\sigma(\beta + 2) + 2\phi\right] = \frac{2\rho_{21}\beta(g - 1)}{S_T}. \tag{C8}$$

The heat balance integral forms for eq C1 and C2 are as follows.

$$\alpha_1\left[\frac{\partial T_1(X,t)}{\partial x} - \frac{\partial T_1(0,t)}{\partial x}\right] - U\left[T_1(X,t) - T_1(0,t)\right] - \frac{d}{dt}\int_0^X T_1(x,t)dx + T_f\frac{dx}{dt} = 0 \tag{C9}$$

$$\alpha_2\left[\frac{\partial T_2(X+\delta,t)}{\partial x} - \frac{\partial T_2(X,t)}{\partial x}\right] - U\left[T_2(X+\delta,t) - T_2(X,t)\right] - \frac{d}{dt}\int_X^{X+\delta} T_2(x,t)dx + T_2(X+\delta)\frac{d(X+\delta)}{dt} - T_f\frac{dX}{dt} = 0. \tag{C10}$$

These two energy equations are summed, along with eq C3, to yield an integrated equation for the entire region undergoing temperature changes. The result is

$$\frac{d}{dt}\left\{\rho_1 c_1\int_0^X T_1(x,t)dx + \rho_2 c_2\int_X^{X+\delta} T_2(x,t)dx - \rho_1 \ell X + (\rho_2 c_2 - \rho_1 c_1)T_f X - \rho_2 c_2(X+\delta)\left[T_o + \frac{G}{2}(X+\delta)\right]\right\}$$

$$= -k_1\frac{\partial T_1(0,t)}{\partial x} + k_2 G - \rho_1 c_1 U\Delta T_1 - \rho_2 c_2 U\left[\Delta T + G(X+\delta)\right]. \tag{C11}$$

Equation C11, the energy integral equation, can now be written nondimensionally as

$$\tau = \int_0^\sigma K_1 d\sigma \tag{C12}$$

$$K_1 = \frac{b_1 + b_2\beta - \frac{1}{6g}\left(1 - \frac{\sigma g'}{g}\right) - C_{21}\sigma\left(\frac{2}{3}\beta + 1\right) - \frac{C_{21}}{3}(\sigma + \phi)\sigma\beta'}{\frac{1}{\sigma}\left(\frac{1}{g} - 2\right) + k_{21} - \psi\left\{1 + 1/S_T + C_{21}\left[\phi + \sigma(\beta + 1)\right]\right\}} \tag{C13}$$

where

$$\psi = \frac{U\Delta T_1}{G\alpha_1}$$

$$b_1 = -\left(\frac{1}{3} + \frac{1}{S_T} + C_{21}\phi\right)$$

$$b_2 = -\frac{1}{3} C_{21}\phi.$$

The derivatives of β and g can be found from the following equations

$$\frac{d\beta}{d\sigma} = \beta' = \frac{a_5 + a_1 a_4}{a_3 + a_2 a_4} \tag{C14}$$

$$\frac{dg}{d\sigma} = g' = a_1 - a_2\beta' \tag{C15}$$

where

$$a_1 = \frac{\alpha_{21}}{m}\left[1 - \frac{(\sigma+\phi)\beta(\beta+2)}{m}\right]$$

$$a_2 = \frac{\alpha_{21}(\sigma+\phi)}{m^2}\left[2\sigma(\beta+1) + 2\phi\right]$$

$$a_3 = \frac{1}{g} - \frac{2\rho_{21}(g-1)}{S_T} - k_{21}\sigma$$

$$a_4 = \left(\frac{2\rho_{21}}{S_T} + \frac{1}{g^2}\right)\beta$$

$$a_5 = k_{21}(\beta+2)$$

$$m = \beta\left[\sigma(\beta+2) + 2\phi\right].$$

The problem has now been reduced to a simple numerical quadrature of eq C12 using the auxiliary relations of eq C13–C15. A FORTRAN program to carry out the integration is listed as PFTSYNB.FOR in Appendix E.

Phase change model verification

A simplification of this problem can be solved in a closed form. Consider the case of a soil initially thawed at T_f and with a zero geothermal gradient G. The problem is then one of a single phase only with eq C1, C1a,b, C3, C4, and C9 governing the freeze process. The temperature is chosen as

$$T = T_f + P\left(\frac{x-X}{X}\right) - \frac{c}{2\ell} P^2 \left(\frac{x-X}{X}\right)^2 \tag{C16}$$

where

$$P = \frac{\ell}{c} R, \qquad R = \sqrt{1 + 2S_T} - 1.$$

The location of the freeze interface is given by

$$t = \frac{K_1}{K_2}\left[X - \frac{K_3}{K_2}\ln\left(\frac{K_2 X + K_3}{K_3}\right)\right] \tag{C17}$$

$$K_1 = 1 + \frac{R}{2}(1 + R/3)$$

$$K_2 = U(1 + S_T)$$

$$K_3 = \alpha R(1 + R).$$

Note that if U is zero, the phase change interface is

$$X^2 = \frac{R(1+R)}{1 + R/2(1 + R/3)} 2\alpha t. \qquad \text{(C18)}$$

Table C1. Comparison of closed solution (G = 0) and numerical quadrature (G = 0.0001).
$S_T = 0.144$, $\alpha = 58.89$ m^2/yr, $\Delta T_1 = 10$°C, $U = 1$ mm/yr.

Freeze depth (m)	*Time (yr) eq C12*	*Time (yr) eq C17*	*Percent difference*
1000	55,867	54,778	1.99
2000	206,996	203,653	1.64
3000	437,935	428,448	2.20

This is identical to the well known Stefan solution given in Lunardini (1991). We may compare the closed form solution (for which $G = 0$) with the numerical quadrature of eq C12 by letting G be very small. Table C1 shows that the results are quite good even for very long freeze times.

Method 2

We can examine the same problem with a different approximation method by referring to Figure 13. For region 3, a quasi-steady approach will be used, leading to a linear temperature profile. The basic equations for heterogenetic growth are valid except that the surface temperature will be replaced by a transient function $T_s'(t)$. Equations 1–5 are valid but the temperature profiles are changed as follows. Quadratic temperature profiles in regions 1 and 2 and a linear temperature in region 3 that satisfy the boundary conditions are

$$T_1 = T_f + a_1 X\left(\frac{x - X}{X}\right) + \left(a_1 X - \Delta T_3\right)\left(\frac{x - X}{X}\right)^2 \qquad \text{(C19)}$$

$$T_2 = T_f + \left[G(\delta + 2X) + 2\Delta T\right]\frac{x - X}{\delta} - (GX + \Delta T)\frac{(x - X)^2}{\delta^2} \qquad \text{(C20)}$$

$$T_3 = T_s + \Delta T_1 MRX\left(\frac{x}{X_d} + 1\right) \qquad \text{(C21)}$$

where

$$a_1 X = \frac{\Delta T_1 M}{g}, \qquad g = \frac{\alpha_{21}(\Delta T + GX)X}{\delta\left[G(\delta + 2X) + 2\Delta T\right]} + 1, \qquad R = \sigma_d k_{13}(2 - 1/g)/\sigma,$$

$$M = \frac{1}{1 + R}, \qquad \Delta T_3 = T_f - T_s'(t) = R\sigma\Delta T_1 M/\left[\sigma_d k_{13}(2 - 1/g)\right].$$

Equation 5 can be used to find a relation between X and δ. In nondimensional form this is

$$\frac{\beta M}{g} - k_{21}\left[\sigma(\beta + 2) + 2\phi\right] = \frac{2\rho_{21}\beta(g - 1)}{S_T}. \qquad \text{(C22)}$$

Equation 3, the energy integral equation, can now be written nondimensionally as

$$\tau = \int_0^\sigma K/H d\sigma \qquad \text{(C23)}$$

$$K = b_1 + (b_2 - A\sigma/3)\beta - M/(6g) - A\sigma/2 + \sigma_d M^2 k_{13}(0.5/g + 1)\left[\left(g'/g^2\right) - (2 - 1/g)/\sigma\right]/3$$

$$+ \sigma\left[(b_2 - A\sigma/3)\beta' + Mg'/\left(6g^2\right) - A(\beta/3 + 0.5)\right]. \qquad \text{(C24)}$$

$$H = \frac{M}{\sigma}(1/g - 2)\left[1 + \psi k_{13} M\sigma(0.5/g + 1)/3\right] + k_{12} \tag{C25}$$

where

$$A = C_{21}, \qquad b_1 = -\left(\frac{M}{3} + \frac{1}{S_t} + C_{21}\phi\right), \qquad b_2 = -\frac{1}{3}C_{21}\phi,$$

$$M = \frac{1}{1+R}, \qquad \sigma_d = \frac{G}{\Delta G_1} X_d.$$

The derivatives of β and g can be found from the following equations

$$\frac{d\beta}{d\sigma} = \beta' = \frac{a_5 + a_1 a_4}{a_3 + a_2 a_4} \tag{C26}$$

$$\frac{dg}{d\sigma} = g' = a_1 - a_2\beta' \tag{C27}$$

where

$$a_1 = \frac{\alpha_{21}}{m}\left[1 - \frac{(\sigma+\phi)\beta(\beta+2)}{m}\right]$$

$$a_2 = \frac{\alpha_{21}(\sigma+\phi)}{m^2}\left[2\sigma(\beta+1) + 2\phi\right]$$

$$a_3 = \frac{M}{g} - \frac{2\rho_{21}(g-1)}{S_T} - k_{21}\sigma + \frac{A\psi k_{13}(2 - 1/g)\beta M^2}{3gH}$$

$$a_4 = \left(\frac{2\rho_{21}}{S_T} + \frac{M}{g^2}\right)\beta + \frac{\beta M^2}{\sigma g^3}\left\{\frac{M\psi k_{13}(2-1/g)\beta M^2}{3gH}\left[(0.5/g+1)M\sigma_d k_{13} + \sigma/2\right] + \sigma_d k_{13}\right\}$$

$$a_5 = k_{21}(\beta+2) + \frac{\beta M^2}{\sigma g}\left[\frac{\sigma_d k_{13}(1-2g)}{\sigma^2 g} + P\right]$$

$$P = \frac{\psi k_{13}(2-1/g)}{\sigma H}\left\{-A\left[\frac{\beta}{3}(2\sigma+\phi) + \sigma + \phi\right] - 1/S_T + \frac{M}{3}(0.5/g+1)\left[\frac{M\sigma_d k_{13}(1-2g)}{\sigma g} - 1\right]\right\}$$

$$m = \beta\left[\sigma(\beta+2) + 2\phi\right].$$

The problem has now been reduced to a simple numerical quadrature of eq C23 using the auxiliary relations of eq C24–C26. A FORTRAN program to carry out the integration is listed in Appendix E as PFTSYN.FOR.

This approximation is inferior to method 1 since the variables in eq C23 are not strictly separable. Nevertheless, predictions for modest times compare quite well to those of method 1.

APPENDIX D: ENERGY FLOWS AT THE PERMAFROST BASE

The heat flows at the base of the permafrost layer determine the rate of movement of the permafrost bottom. Examine Figure D1 to clarify the concepts involved. At any instant of time, an amount of energy, $q_f(t)$, is conducted away from the phase-change interface through the frozen layer and to the interface from the thawed zone 2, q_u. It is important to realize that the constant geothermal heat flow $q_g = k_u G$ will only equal $q_u(t)$ at equilibrium. During movement of the permafrost base, $q_u(t)$ can be greater or less than q_g. We can examine the transient behavior of these terms. Let

$$Q_f = \frac{q_f(t)}{k_u G} = \frac{k_f}{k_u}\frac{1}{G}\frac{\partial T_1(X,t)}{\partial x} \qquad \text{(D1)}$$

$$Q_u = \frac{q_u(t)}{k_u G} = \frac{1}{G}\frac{\partial T_2(X,t)}{\partial x}. \qquad \text{(D2)}$$

In terms of dimensionless parameters

$$Q_f = \frac{1}{\sigma k_{21}\left\{\dfrac{\alpha_{21}(\sigma+\phi)}{\beta[\sigma(\beta+2)+2\phi]}+1\right\}} \qquad \text{(D3)}$$

$$Q_u = \frac{\sigma(\beta+2)+2\phi}{\sigma\beta} \qquad \text{(D4)}$$

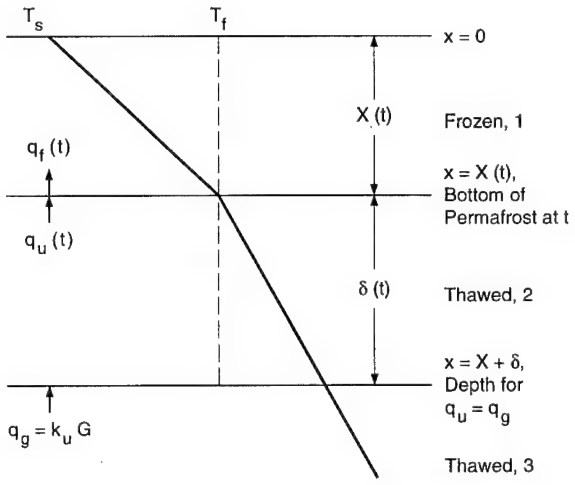

Figure D1. Energy flows at base of permafrost.

where we assume that $k_u = k_2$, i.e., the thermal conductivity of the thawed zone is constant. The results of example 2 for Prudhoe Bay are tabulated in Table D1. Clearly, the heat flow from the deep layer greatly exceeds the geothermal heat flow for much of the permafrost formation period. Also, note how rapidly the heat flow out of the frozen zone Q_f drops to slightly more than the flow from the thawed layer Q_u.

The temperature in the frozen zone adjusts very quickly toward the equilibrium result of a linear temperature distribution; however, the thermal zone approaches equilibrium very slowly.

Surface temperature increase

Suppose the permafrost has thickness X_o, is growing and the surface temperature initially increases by a certain amount and is held constant for several thousand years. What is the effect on the permafrost? The bottom of the permafrost will continue to grow for several hundred years before starting to thaw, but Table D1 assures us that this will be negligible. At t = 225,000 years, X_o = 626.5 m and the permafrost growth will only be 27.5 cm during the next 1000 years. Thus, we can assume that the permafrost thickness remains essentially constant while the temperature in the frozen zone

Table D1. Freeze at Prudhoe Bay, Alaska.

ΔT_1 = 12.69°C ϕ = 0
k_{21} = 0.5812 S_T = 0.1827
α_{21} = 0.3915 X_e = 763.5 m

Time (yr)	*Permafrost depth (m)*	β	Q_u	Q_f	$\frac{q_f}{q_{fe}} = \frac{1}{\frac{\alpha_{21}}{\beta(\beta+2)}+1}$
1	4.44	1.9060	2.423	159.057	0.9251
350	79.9	1.6717	2.196	8.986	0.9405
3500	219.3	2.3380	1.855	3.352	0.9629
35,000	461.4	4.8154	1.4153	1.6351	0.9826
100,000	567.8	7.7133	1.2593	1.3375	—
225,000	626.5	11.1633	1.1792	1.2153	—
775,000	687.7	20.3168	1.0984	1.1090	—

adjusts to its new equilibrium value. Figure D2 sketches the problem. Obviously, after infinite time the new temperature profile is as shown. However, the temperature will adjust to near the new equilibrium in a relatively short time. This is a linear problem in non-phase-change conduction and has been solved by Lachenbruch et al. (1982). The transient temperature is

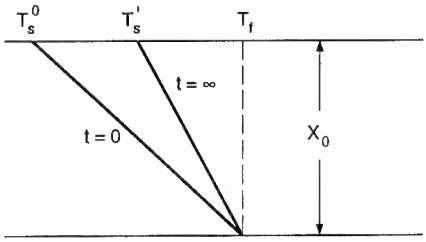

Figure D2. Permafrost equilibrium temperature profiles.

$$T = T_s' + (T_f - T_s')\frac{x}{X_0} + \frac{2}{\pi}(T_s^o - T_s')\sum_{n=1}^{\infty}\frac{1}{n}e^{-M}\sin\left(n\pi\frac{x}{X_0}\right) \quad \text{(D5)}$$

where

$$M = \frac{n^2\pi^2 t}{4t_c}, \qquad t_c = \frac{X_0^2}{4\alpha_f}.$$

t_c is a characteristic time for sensible temperature changes. The equilibrium temperatures are simply

$$T_0 = T_s^o + (T_s - T_s^o)\frac{x}{X_0} \quad \text{(D6)}$$

$$T_\infty = T_s' + (T_f - T_s')\frac{x}{X_0}. \quad \text{(D7)}$$

The change in sensible heat, going from the state at $t = 0$ to the state at $t = \infty$, is

$$Q_{s\infty} = C_f(T_s' - T_s^o)\frac{X_0}{2}. \quad \text{(D8)}$$

The change in sensible heat at any time t is

$$Q_s = C_f\int_0^{X_0}(T - T_0)dx = Q_{s\infty} + \frac{2C_f}{\pi^2}(T_s^o - T_s')X_0\sum_{n=1}^{\infty}\frac{e^{-M}}{n^2}\left[1-(-1)^n\right]. \quad \text{(D9)}$$

Thus, the relative change in sensible heat is

$$\frac{Q_{s\infty} - Q_s}{Q_{s\infty}} = \frac{4}{\pi^2}\sum_{n=1}^{\infty}\frac{e^{-M}}{n^2}\left[1-(-1)^n\right]. \quad \text{(D10)}$$

Note that this quantity does not depend upon the surface temperatures. The relative change is shown in Table D2. The sensible heat change attains 93% of its ultimate value at $t/\lambda = 1.0$ ($t = 1666$ years) and 99% at $t/\lambda = 1.78$ ($t = 2966$ years). The sensible heat changes would be essentially completed after about 1670 years. From this time on, the bottom of the permafrost would slowly melt.

Change in frozen zone temperature gradient at bottom of permafrost

The time required for the temperature gradient, in the frozen zone, to change is important since this quantity will determine the rate of change of the permafrost bottom depth. The gradient at the depth X_0 can be found from eq D5 and is

$$\delta = \left.\frac{\partial T}{\partial x}\right|_{x=X_0} = \frac{T_f - T_s'}{X_0} + \frac{2}{X_0}(T_s^o - T_s')\sum_{n=1}^{\infty}(-1)^n e^{-M}. \quad \text{(D11)}$$

Table D2. Relative change in sensible heat.

t/λ	$\frac{Q_{s\infty} - Q_s}{Q_{s\infty}}$
0.25	0.438
0.50	0.236
1.0	0.069
1.50	0.020
1.78	0.010
2.0	0.006

The initial temperature gradient, at $x = X_o$, is

$$\delta^o = \frac{\partial T}{\partial x}(X_o, 0) = \frac{T_f - T_s^o}{X_o}. \qquad \text{(D12)}$$

Note that this simplified form of δ^o gives virtually the same heat flux as the value from eq D1, when $x = X_o$. Now

$$\frac{\delta^o - \delta}{\delta^o} = \frac{T_s' - T_s^o}{T_f - T_s^o}\left[1 + 2\sum_{n=1}^{\infty}(-1)^n e^{-M}\right]. \qquad \text{(D13)}$$

The time for a given change in the gradient can be closely approximated as

$$\frac{t}{\lambda} = \frac{4}{\pi^2}\ln\left[\frac{2}{1 - \left(\frac{\delta^o - \delta}{\delta}\right)\left(\frac{T_f - T_s^o}{T_s' - T_s^o}\right)}\right]. \qquad \text{(D14)}$$

Table D3. Time for change in gradient.

$T_s^o = -13.69°C$; $T_s' = -11.0$; $T_f = -1.0$

$\frac{\delta^o - \delta}{\delta}$	t/λ	t *(years)*	$\left(\frac{\delta^o - \delta}{\delta}\right)^*$
0.01	0.301	502	0.0314
0.0297	0.3421	570	0.0440
0.1	0.540	899	0.1022
0.20	1.446	2408	0.20
0.212	∞	∞	—

* Calculated without eq D14 approximation.

Table D3 shows the results for Prudhoe Bay.

It would take about 490 years for the bottom growth to cease and 900 years for the bottom gradient to change significantly. Thus, the approximations used in the derivation of eq D5 are acceptable.

Bottom melt

The temperature in the frozen zone requires 1666 years for sensible heat adjustment, leaving $\Delta t = 15000 - 1666 = 13{,}334$ years for bottom melt (the interglacial is 15,000 years long). The energy balance at the bottom of the permafrost is

$$L\frac{dX}{dt} = k_f\frac{T_f - T_s'}{X} - Aq_g. \qquad \text{(D15)}$$

where A is the fraction of the geothermal energy that goes into melting; it can exceed 1.0.

The heat flow from the thawed zone is greater than the geothermal heat flow, as we have seen. For the example discussed here, $A = 1.179$ at the beginning of thaw and will decline towards 1 as thaw proceeds. The permafrost thickness X_f after Δt years is given by

$$X_f - b\,\ln\left(\frac{X_f + b}{X_o + b}\right) = a + X_o \qquad \text{(D16)}$$

where

$$a = -A\frac{q_g \Delta t}{L}, \qquad b = -\frac{k_f(T_f - T_s')}{Aq_g}, \qquad q_g = k_u G.$$

Table D4. Permafrost thickness.*

A	X_f *(m)*
1.179	591.0
1.0895	605.5
1.0	620.0

*Final thickness after surface temperature increase, Prudhoe Bay.

The final permafrost thickness is strongly dependent upon the value of A. Table D4 shows values for the Prudhoe Bay example.

The heat flow from the thawed zone varies continuously during the thaw, denoted in eq D15 as $A(t)\,q_g$. The heat flow at equilibrium is such that $A = A_e = 1.0$. Thus, let $A(t)$ be a linear function of X, given by

$$A = (A_o - A_e)\left(\frac{y - y_e}{1 - y_e}\right) + A_e \qquad \text{(D16a)}$$

where $y = X/X_o$

A_o = value at thaw commencement

A_e = equilibrium value

$X_e = \dfrac{T_f - T_s'}{k_{uf} G}$ = new equilibrium permafrost thickness.

Equation D15 then has the following solution

$$\ln\left(\frac{a_1 y_f^2 + a_2 y_f - 1}{a_1 + a_2 - 1}\right) - \frac{a_2}{a_3}\ln\left[\left(\frac{y_f + a_4}{y_f + a_5}\right)\left(\frac{1 + a_5}{1 + a_4}\right)\right] + 2a_1\tau_f = 0 \qquad \text{(D17)}$$

where

$$a_1 = \frac{q_g X_o}{k_f\left(T_f - T_s'\right)} \frac{\left(A_o - A_e\right)}{\left(1 - y_e\right)}$$

$$a_2 = A_e - y_e \frac{\left(A_o - A_e\right)}{\left(1 - y_e\right)}$$

$$a_3 = \sqrt{a_2^2 + 4a_1}$$

$$a_4 = \frac{a_2 - a_3}{2a_1}$$

$$a_5 = \frac{a_2 + a_3}{2a_1}$$

$$\tau_f = \frac{k_f\left(T_f - T_s'\right)\Delta t}{L X_o^2}$$

and

$$y_f = \frac{X_f}{X_o}$$

is the permafrost thickness after Dt years (Table D5).

Note that these results agree quite well with the values with a constant thawed zone heat flow, i.e., constant value of $A(t)$. For this case, 15,000 years is nearly enough time to thaw back to the new equilibrium thickness of 601.5 m.

Table D5. Permafrost thickness after thaw.

A_o = 1.1792.

A_e	y_f	X_f (m)
1.0	0.9678	606.4
1.170	0.945	592.0
1.179	0.9434	591.0

APPENDIX E: FORTRAN PROGRAMS FOR NUMERICAL QUADRATURE OF ENERGY EQUATION

Program PERM

```
C     $DECLARE
C     $DEBUG
Ccc   10 REM  **********  PERM   **********
CCC   REAL A21,BET,C21,EP,K,K21,PHI,R21,R,ST,Y,B1,B2,B3,B4
CCC   REAL D,DELS,DELTATO,DELTAT1,G,GG,SIGI,SIGF,XI
CCC   REAL A1,A2,A3,A4,A5,TAU,X,T,B,BPP,GP,GPP,F,H,FP
      IMPLICIT DOUBLE PRECISION (A-H,K-M,O-Z)
      COMMON /DATA/ A21,BET,K,K21,PHI,R21,R,ST,Y,B1,B2,B3
      character PRNTR*12
      integer i,j,n
c
      PRNTR = 'OUT.DAT'
2      OPEN(9,FILE=PRNTR, STATUS='NEW')
c
C ******** INPUT VALUES ******************
      ST = 0.143960
      EP = 0.379
      KI = 5.45
      KW = 1.34
      KG = 10.360
      GAM = .9825

C ****** CALCULATED VALUES ***********

      KWI = KW/KI
      K21 = ((KWI)**EP)*((GAM)**(1.0-EP))
      C21 = (.9357 + 1.243*EP)/(.9155+.0845*EP)
      A21 = K21/C21
      R21 = (2.6-1.6*EP)/(2.6-1.69*EP)
      K1 = ((KI)**EP)*((KG)**(1.0-EP))
      C1 = .4202+.0388*EP
      AL1 = 3.1536*K1/C1
      L = 79.71*EP

      DELTATO = 0.0
      DELTAT1 = L*ST/C1

C ****** INCREMENT FOR SIMPSON *******

      DELS = 0.00005
      D = DELS/100.
      GG = 0.0286
      BET = 1.0
      R = 0.33330
      PHI = DELTATO/DELTAT1
      SIGI = 1.0/K21
      SIGF = 0.9*SIGI
      XI = DELTAT1/(GG*K21)
      B3 = K21/A21
      B1 = -(1.0/3.0 + 1./ST + B3*PHI)
      B2 = -B3*PHI/3.0
      B4 = SIGI/DELS
      N = B4

130   Write(9,3000)
```

```
3000  format(1x,'          TIME OF PERMAFROST FORMATION ')
137   Write(9,3015)  EP
3015  format(1x,' VOID RATIO EPSILON                = ',F9.4)
140   Write(9,3001)  ST
3001  format(1x,' STEFAN NUMBER, C1*DELTAT1/L       = ',F9.4)
141   Write(9,3004)  R
3004  format(1x,' SUSPECT CONSTANT                  = ',F9.4)
150   Write(9,3002)  K21
3002  format(1x,' THAW/FROZEN CONDUCTIVITY RATIO    = ',F9.4)
138   Write(9,3016)  C21
3016  format(1x,' THAW/FROZEN HEAT CAPACITY RATIO   = ',F9.4)
160   Write(9,3003)  A21
3003  format(1x,' THAW/FROZEN DIFFUSIVITY RATIO     = ',F9.4)
      Write(9,3013)  R21
3013  format(1x,' THAW/FROZEN DENSITY RATIO         = ',F9.4)
      Write(9,5)  KG
5     format(1x,' SOIL SOLIDS KG MCAL/(S-CM-C)      = ',F9.4)
      Write(9,3021)  K1
3021  format(1x,' FROZEN K MCAL/(S-CM-C)            = ',F9.4)
      Write(9,3022)  C1
3022  format(1x,' FROZEN C CAL/(CM**3-C)            = ',F9.4)
      Write(9,3023)  AL1
3023  format(1x,' FROZEN ALPHA M**2/YEAR            = ',F9.4)
      Write(9,3024)  L
3024  format(1x,' LATENT HEAT CAL/CC                = ',F9.4)
      Write(9,3014)  DELTAT0
3014  format(1x,' (TO - TF) DEGREE C                = ',F9.4)
180   Write(9,3005)  DELTAT1
3005  format(1x,' (TF - TS) DEGREE C                = ',F9.4)
191   Write(9,3007)  GG
3007  format(1x,' GEOTHERMAL GRADIENT DEG C/M       = ',F9.4)
200   Write(9,3008) D
3008  format(1x,' INCREMENT FOR SIMPSON             = ',F9.4)
201   Write(9,3009) PHI
3009  format(1x,' PHI = (TO - TF)/(TF - TS)         = ',F9.4)
202   Write(9,3010)  SIGI
3010  format(1x,' EQUIBRIUM FREEZE DEPTH            = ',F9.4)
203   Write(9,3019)  SIGF
3019  format(1x,' 90 % EQUIBRIUM FREEZE DEPTH       = ',F9.4)
210   Write(9,3011)  XI
3011  format(1x,' EQUIBRIUM FREEZE DEPTH  METERS    = ',F9.4)


      TAU = 0.0
      X = 0.0
222   Write(9,*)
252   Write(9,*) '       TIME       SIGMA      BETA
253   Write(9,2001) TAU, X, BET
2001  format(1x,F13.4,2F10.4)

260   DO 80, I=1,N
      TS = X
      TE = X + DELS
      IF(X .EQ. 0.0) GO TO 10
      Y = TS
      CALL BETA
      KS = K
11    Y = TS +D
      SO = 0.0
      DO 20 J =1,50
      CALL BETA
      SO = SO + K
      Y=Y+2*D
20    CONTINUE
      SOO = 4*SO
      Y = TS+2.0*D
      SE = 0.0
      DO 30 JJ = 1,49
      CALL BETA
      SE = SE+K
      Y = Y+2.0*D
30    CONTINUE
      SOE = 2.0*SE
      Y = TE
```

```
      CALL BETA
      KE = K
      S1 = KS+KE
      T = D*(S1+SOO+SOE)/3.0
      TAU = TAU+T
      X = X + DELS
131   Write(9,*)
133   Write(9,2001) TAU, X, BET
80    CONTINUE
      GO TO 1850

10    KS = 0.0
      GO TO 11
1850  END

      SUBROUTINE BETA
      IMPLICIT DOUBLE PRECISION (A-H,K-M,O-Z)
      COMMON /DATA/ A21,BET,K,K21,PHI,R21,R,ST,Y,B1,B2,B3

40    BET = BET
      M = Y*(BET+2.0)+2.0*PHI
      G = A21*(Y+PHI)/(BET*M)+1.0
      GP = -A21*(Y+PHI)*(M+BET*Y)/((BET*M)**2)
      B = BET/G - M*K21 - 2.0*R21*BET*(G-1.0)/ST
      BP = (1.0-BET*GP/G)/G - K21*Y +2.0*R21*A21*Y*(Y+PHI)/(ST*(M**2))
      BET1 = BET - B/BP
      IF(ABS(BET1-BET) .LT. 0.01) GO TO 50
      BET = BET1
      GO TO 40
50    BET = BET1
      M = Y*(BET+2.0)+2.0*PHI
      G = A21*(Y+PHI)/(BET*M)+1.0
      A1 = A21*(1.0-(Y+PHI)*(BET+2.0)/M)/(M*BET)
      A2 = 2.0*A21*(Y+PHI)*(Y*(BET+1.0)+PHI)/((M*BET)**2)
      A3 = 1.0/G - 2.0*R21*(G-1.0)/ST - K21*Y
      A4 = (2.0*R21/ST+1.0/(G**2))*BET
      A5 = K21*(BET+2.0)
      BPP = (A5+A1*A4)/(A3+A2*A4)
      GPP = A1 - A2*BPP
      F = B1+(B2-B3*Y/3)*BET-1.0/(6*G)-B3*Y/2.0
      H = (1.0/G-2.0)/Y+K21
      FP = (B2-B3*Y/3)*BPP+GPP/(6*(G**2))-B3*(BET/3+.5)
      K = (F+Y*FP)/H
      RETURN
      END
```

Program PFTSYN

```
C     $DECLARE
C     $DEBUG
Ccc   10 REM  **********  PFTSYN   **********
CCC   REAL A21,BET,C21,EP,K,K21,K13,PHI,R21,R,ST,Y,B1,B2,B3,B4
CCC   REAL D,DELS,DELTATO,DELTAT1,G,GG,PSI,SIGD,SIGI,SIGF,SIGL,U,XI
CCC   REAL A,A1,A2,A3,A4,A5,TAU,X,XD,XP,XT,T,B,BPP,BPA,GP,GPP,F,H,FP
CCC   REAL S1,S2,S3,MN,H1,Q1,Q2,Q3,Q4,Q5,Q6,Q12,Q13,Q14,Q15
      IMPLICIT DOUBLE PRECISION (A-H,K-M,O-Z)
      COMMON /DATA/ A,A21,BET,K,K21,K13,XD,PHI,PSI,R21,R,ST,Y,B1,B2,B3
      character PRNTR*12
      integer i,j,n
c
      PRNTR = 'OUT.DAT'
2      OPEN(9,FILE=PRNTR, STATUS='NEW')
c
C ******** INPUT VALUES ******************
      ST = .143960250
      EP = 0.379
      KI = 5.45
      KW = 1.34
      KG = 10.360
      GAM = .9825
      U = 10.0
      K13 = 1.0
```

```
C ****** CALCULATED VALUES ***********

      KWI = KW/KI
      K21 = ((KWI)**EP)*((GAM)**(1.0-EP))
      C21 = (.9357 + 1.243*EP)/(.9155+.0845*EP)
      A21 = K21/C21
      R21 = (2.6-1.6*EP)/(2.6-1.69*EP)
      K1 = ((KI)**EP)*((KG)**(1.0-EP))
      C1 = .4202+.0388*EP
      AL1 = 3.1536*K1/C1
      L = 79.71*EP

C     K21 = 1.0
C     C21 = 1.0
C     A21 = 1.0
C     R21 = 1.0
C     ST = 1000.
      A=C21
      DELTAT0 = 0.0
      DELTAT1 = L*ST/C1
C     DELTAT1 = 10.0

C ****** INCREMENT FOR SIMPSON *******

      DELS = 0.00005
      D = DELS/100.
      GG = 0.0286
      PSI = U*.001*DELTAT1/(AL1*GG)
      BET = 1.0
      PHI = DELTAT0/DELTAT1
      SIGI = 1.0/K21
      SIGF = 0.9*SIGI
      SIGL = SIGI-0.01
      XI = DELTAT1/(GG*K21)
      B3 = K21/A21
      B1 = -(1.0/3.0 + 1./ST + B3*PHI)
      B2 = -B3*PHI/3.0
      B4 = SIGI/DELS
      N =B4

130   Write(9,3000)
3000  format(1X,' TIME OF SYNGENETIC PERMAFROST FORMATION ')
137   Write(9,3015)  EP
3015  format(1x,' VOID RATIO EPSILON              = ',F9.4)
140   Write(9,3001)  ST
3001  format(1x,' STEFAN NUMBER, C1*DELTAT1/L    = ',F9.4)
141   Write(9,3004)  U
3004  format(1x,' DEPOSITION RATE MM/YR          = ',F9.4)
129   Write(9,2999)  PSI
2999  format(1x,' DEPOSITION PARAMETER PSI       =   ',F9.6)
150   Write(9,3002)  K21
3002  format(1x,' THAW/FROZEN CONDUCTIVITY RATIO  = ',F9.4)
138   Write(9,3016)  C21
3016  format(1x,' THAW/FROZEN HEAT CAPACITY RATIO = ',F9.4)
160   Write(9,3003)  A21
3003  format(1x,' THAW/FROZEN DIFFUSIVITY RATIO   = ',F9.4)
      Write(9,3013)  R21
3013  format(1x,' THAW/FROZEN DENSITY RATIO       = ',F9.4)
      Write(9,5)  KG
5     format(1x,' SOIL SOLIDS KG MCAL/(S-CM-C)    = ',F9.4)
      Write(9,3021)  K1
3021  format(1x,' FROZEN K MCAL/(S-CM-C)          = ',F9.4)
      Write(9,3022)  C1
3022  format(1x,' FROZEN C CAL/(CM**3-C)          = ',F9.4)
      Write(9,3023)  AL1
3023  format(1x,' FROZEN ALPHA M**2/YEAR          = ',F9.4)
      Write(9,3024)  L
3024  format(1x,' LATENT HEAT CAL/CC              = ',F9.4)
      Write(9,3014)  DELTAT0
3014  format(1x,' (TO - TF) DEGREE C              = ',F9.4)
180   Write(9,3005)  DELTAT1
3005  format(1x,' (TF - TS) DEGREE C              = ',F9.4)
191   Write(9,3007)  GG
3007  format(1x,' GEOTHERMAL GRADIENT DEG C/M     = ',F9.4)
200   Write(9,3008) DELS
3008  format(1x,' INCREMENT FOR SIMPSON           = ',F9.6)
201   Write(9,3009) PHI
```

```
3009  format(1x,' PHI = (TO - TF)/(TF - TS)       = ',F9.4)
202   Write(9,3010)  SIGI
3010  format(1x,' EQUIBRIUM FREEZE DEPTH          = ',F9.4)
203   Write(9,3019)  SIGF
3019  format(1x,' 90 % EQUIBRIUM FREEZE DEPTH     = ',F9.4)
210   Write(9,3011)  XI
3011  format(1x,' EQUIBRIUM FREEZE DEPTH  METERS  = ',F9.4)
      TAU = 0.0
      X = 0.0
      XD = 0.0
      XP = 0.01

      XT=X+XD
222   Write(9,*)
252   Write(9,*) '       TIME      SIGMA      BETA       SIGD       SIGT
253   Write(9,2001) TAU, X, BET,XD,XT
2001  format(1x,F13.4,4F10.4)

260   DO 80 I=1,N
      TS = X
      TE = X + DELS
      IF(X .EQ. 0.0) GO TO 10
      Y = TS
      CALL BETA
      KS = K
11    Y = TS +D
      SO = 0.0
      DO 20 J =1,50
      CALL BETA
      SO = SO + K
      Y=Y+2*D
20    CONTINUE
      SOO = 4*SO
      Y = TS+2.0*D
      SE = 0.0
      DO 30 JJ = 1,49
      CALL BETA
      SE = SE+K
      Y = Y+2.0*D
30    CONTINUE
      SOE = 2.0*SE
      Y = TE
      CALL BETA
      KE = K
      S1 = KS+KE
      T = D*(S1+SOO+SOE)/3.0
      IF(T .LT. 0.0) GO TO 131
      TAU = TAU+T
      X = X + DELS
      XD = XD+PSI*T
      XT = XD+X
      IF(XT .GT. SIGL) GO TO 131
      IF(X .LT. XP) GO TO 80
      XP =XP +0.01
131   Write(9,*)
133   Write(9,2001) TAU, X, BET, XD, XT
      IF(XT .GT. SIGL) GO TO 1850
      IF(T .LT. 0.0) GO TO 1850
80    CONTINUE
      GO TO 1850
10    KS = 0.0
      GO TO 11
1850  END

      SUBROUTINE BETA
      IMPLICIT DOUBLE PRECISION (A-H,K-M,O-Z)
      COMMON /DATA/ A,A21,BET,K,K21,K13,XD,PHI,PSI,R21,R,ST,Y,B1,B2,B3

40    BET = BET
      M = Y*(BET+2.0)+2.0*PHI
      G = A21*(Y+PHI)/(BET*M)+1.0
      R = K13*XD*(2.-1./G)/Y
      GP = -A21*(Y+PHI)*(M+BET*Y)/((BET*M)**2)
      B = BET/G - M*K21 - 2.0*R21*BET*(G-1.0)/ST-R*BET/((1.+R)*G)
      P1 = 1.0/((1.+R)*(2.*G-1.))
      P = R/((1.0+R)*G)
```

```
      BPA=P+P*BET*GP*(P1-1.)/G
      BP=(1.0-BET*GP/G)/G-K21*Y+2.0*R21*A21*Y*(Y+PHI)/(ST*(M**2))-BPA
      BET1 = BET - B/BP
      IF(ABS(BET1-BET) .LT. 0.01) GO TO 50
      BET = BET1
      GO TO 40
50    BET = BET1
      M = Y*(BET+2.0)+2.0*PHI
      G = A21*(Y+PHI)/(BET*M)+1.0
      R = K13*XD*(2.-1./G)/Y
      A1 = A21*(1.0-(Y+PHI)*(BET+2.0)/M)/(M*BET)
      A2 = 2.0*A21*(Y+PHI)*(Y*(BET+1.0)+PHI)/((M*BET)**2)
      S1=-A*(BET*(Y+PHI)/3.+Y/2.+PHI)-1./ST
      S2=K13*(2.-1./G)/Y
      S3=0.5/G+1.0
      MN=1./(1.0+R)
      H1=MN*(1./G-2.)/Y+K21-Y*S3*(MN**2)*PSI*S2/3.
      Q12=S3*(MN**2)*XD*K13/(3.*G)
      Q1=S1-MN*S3/3.+Q12*(1.-2.*G)/Y-Y*A*(BET/3.+.5)
      Q2=Q12/G+MN*Y/(6.*(G**2))
      Q3=Y*A*(Y+PHI)/3.
      Q13=PSI*S2/H1
      Q14=BET*(MN**2)/G
      Q4=-Q14*(Q13*Q1+XD*K13*(1.-2.*G)/((Y**2)*G))
      Q5=-Q14*(Q13*Q2+XD*K13/(Y*(G**2)))
      Q6=Q14*Q3*Q13
      Q15=2.*R21/ST
      A3 = MN/G - Q15*(G-1.0) - K21*Y+Q6
      A4 = Q15*BET+1.0/(G**2)*BET*MN-Q5
      A5 = K21*(BET+2.0)-Q4
      BPP = (A5+A1*A4)/(A3+A2*A4)
      GPP = A1 - A2*BPP
      K = (Q1+Q2*GPP-Q3*BPP)/H1
      RETURN
      END
```

REPORT DOCUMENTATION PAGE

Form Approved
OMB No. 0704-0188

1. AGENCY USE ONLY (Leave blank)	2. REPORT DATE	3. REPORT TYPE AND DATES COVERED
	April 1995	

4. TITLE AND SUBTITLE

Permafrost Formation Time

5. FUNDING NUMBERS

PR: 4A161102AT24
TA: BS/0045

6. AUTHORS

Virgil J. Lunardini

7. PERFORMING ORGANIZATION NAME(S) AND ADDRESS(ES)

U.S. Army Cold Regions Research and Engineering Laboratory
72 Lyme Road
Hanover, New Hampshire 03755-1290

8. PERFORMING ORGANIZATION REPORT NUMBER

CRREL Report 95-8

9. SPONSORING/MONITORING AGENCY NAME(S) AND ADDRESS(ES)

Office of the Chief of Engineers
Washington, DC 20314-1000

10. SPONSORING/MONITORING AGENCY REPORT NUMBER

11. SUPPLEMENTARY NOTES

Funding also provided by U.S. Army Strategic Environmental Research and Development Program 2.6.00 78 203

12a. DISTRIBUTION/AVAILABILITY STATEMENT

Approved for public release; distribution is unlimited.

Available from NTIS, Springfield, Virginia 22161.

12b. DISTRIBUTION CODE

13. ABSTRACT (*Maximum 200 words*)

The age of permafrost is closely linked to the time required for soil systems to freeze, since the permafrost must be at least as old as the formation time. Cycles of freeze–thaw will complicate the relation between the freeze rate and the age. A model based on pure conduction heat transfer with freeze–thaw is used to predict the time required for a given thickness of permafrost to develop, either heterogenetically or syngenetically. The formation time is a function of the long-term geothermal gradient (initial temperature of the thawed soil), the ratios of the frozen to thawed thermal properties, and the temperature history of the upper surface of the permafrost (higher than the air temperature). The simple theory allows universal graphs to be produced that predict the formation time for a given thickness of permafrost. Realistic soil property ratios and paleotemperature scenarios will then lead to estimates of the formation time of permafrost for a specific site. The model indicates that deep permafrost (more than 1500 m) requires formation times on the order of the complete Quaternary Period.

14. SUBJECT TERMS

Age of permafrost
Paleotemperatures
Permafrost
Permafrost growth and melt

15. NUMBER OF PAGES

48

16. PRICE CODE

17. SECURITY CLASSIFICATION OF REPORT	18. SECURITY CLASSIFICATION OF THIS PAGE	19. SECURITY CLASSIFICATION OF ABSTRACT	20. LIMITATION OF ABSTRACT
UNCLASSIFIED	UNCLASSIFIED	UNCLASSIFIED	